Unraveling the Direct Decomposition of NO x over Keggin Heteropolyacids and Their Deactivation Using a Combination of Gas-IR/MS and In Situ DRIFT Spectroscopy

Josefine Schnee, Laurent Delannoy, Guylène Costentin, Cyril Thomas

HAL Id: hal-02960399
https://hal.sorbonne-universite.fr/hal-02960399

Submitted on 7 Oct 2020

Unravelling the Direct Decomposition of NO$_x$ over Keggin Heteropolyacids and their Deactivation Using a Combination of Gas-IR/MS and *in Situ* DRIFT

Josefine Schnee,* Laurent Delannoy, Guylène Costentin, and Cyril Thomas*

Sorbonne Université, CNRS, Laboratoire de Réactivité de Surface (LRS), F-75005 Paris, France.

*Corresponding authors: josefine.schnee@upmc.fr, josischnee@hotmail.com, cyril.thomas@upmc.fr.

Abstract

Keggin heteropolyacids (HPAs) have been known to be efficient NO$_x$ absorbers for many years, and to decompose a significant fraction of the NO$_x$ species pre-absorbed at 100-150 °C into harmless N$_2$ and O$_2$ upon rapid heating to 450 °C. However, this capability of Keggin HPAs to directly decompose NO$_x$ in the absence of reducing agent in the feed has never been studied under more realistic reaction conditions, e.g. under continuous NO$_x$ feeding and in the presence of O$_2$ in the feed. This was done for the first time in the present work, over the widely used H$_3$PW$_{12}$O$_{40}$ Keggin HPA, at 380 °C. H$_3$PW$_{12}$O$_{40}$ was shown to be active in the direct decomposition of continuously fed NO$_x$, with the decomposition process occurring through the involvement of NOH$^+$ adspecies. O$_2$ was found to play a dual role. On the one hand, it led to the oxidation of NO into NO$_2$ in the feed, with NO$_2$ deactivating the HPA units. On the other hand, it was found to initiate the diffusion of NO$_x$ into the bulk of the HPA crystals, which significantly enhanced the durability of the activity of the HPA in the direct decomposition of these NO$_x$, provided that the diffusion pathway in-between the bulk Keggin units was already accessible thanks to the presence of NO$_x$ species pre-absorbed at RT. By providing the key factors involved in the direct decomposition of continuously fed NO$_x$ over H$_3$PW$_{12}$O$_{40}$, the present work paves the way for future investigations that might focus, for instance, on tuning the chemical composition of the heteropolyanions in order to make the HPA more resistant to deactivation.

1. Introduction

Heteropolyacids (HPAs) are metal-oxygen clusters which have a discrete ionic structure consisting of mobile elementary units, namely heteropolyanions and protons. This mobility is the source of very interesting catalytic properties.[1,2] HPAs exhibit unique redox properties which can be tuned by varying their chemical composition.[1,3] They also exhibit a very strong Brönsted acidity, being much stronger than that of conventional inorganic acids, and approaching the super-acid region.[1,4,5] Among a large diversity of structures, Keggin HPAs are the most studied. Indeed, they are the most stable and the most easily available ones.[2,6] The Keggin unit is composed of a heteropolyanion having the formula [XM$_{12}$O$_{40}$]$^{n-}$ (typically, X = P or Si and M = W or Mo) and being stabilized by n acidic protons.[6] The heteropolyanion is made of a central XO$_4$ tetrahedron, surrounded by 12 MO$_6$ octahedra.[7] It contains 3 types of oxygen atoms: central (O$_a$), bridging, and terminal (O$_d$) ones. The bridging ones are either corner-sharing (O$_b$) or edge-sharing (O$_c$). In the hydrated solid, Keggin units are coordinated with

structural water molecules. Most commonly, six structural water molecules are contained per Keggin unit, forming a body-centered cubic structure with Keggin anions at the lattice points and acidic $H_5O_2^+$ bridges along the faces.[2,8]

Keggin HPAs are known to be highly efficient absorbers of nitrogen oxides (NO_x) being among the major pollutants of the atmosphere.[9] NO_x largely contribute to current environmental issues such as photochemical smog, acid rain, tropospheric ozone, ozone layer depletion and global warming.[10,11,12] At 100-150 °C, the constitutive crystals of Keggin HPAs are reported to accommodate NO and NO_2 within their bulk, thus in-between the $[XM_{12}O_{40}]^{n-}$ heteropolyanions, as NOH^+ and HNO_2^+ moieties.[9] Upon rapid heating (150 °C/min) to 450 °C under inert atmosphere, about 70% of the pre-absorbed NO_x species are decomposed into harmless N_2 and O_2.[9] The term "absorption" refers here to the diffusion of NO_x into the bulk of the HPA crystals, in which NO_x adsorb as NOH^+ and HNO_2^+ species onto the surface of the constitutive heteropolyanions. It does not refer to the diffusion of NO_x into the bulk of the Keggin units themselves. The mechanism of the NO_x decomposition process is still unclear. It is however generally accepted to involve the protons of the HPA.[9]

Although the capability of Keggin HPAs to directly decompose NO_x in the absence of reducing agent in the feed has been known for 25 years, it has, to our knowledge, never been studied under more realistic reaction conditions, e.g. under continuous NO_x feeding and in the presence of O_2 in the feed. However, the catalytic direct NO_x decomposition is nowadays considered as offering an ideal solution to the abatement of NO_x from the exhausts of automotive and various combustion processes.[10,12,13] The development of efficient formulations, classically based on noble metals, metal oxides or zeolites, is of the utmost interest to meet the ever more stringent emission regulations.[10,11,12,14,15,16,17] As a reference, over Cu-ZSM-5 being among the most active and stable catalysts reported for direct NO decomposition, NO decomposition rates of 0.134 and 8.16 μmol/$g_{catalyst}$/s have been obtained with Cu(wt%) of 0.76 and 3.88, respectively, in the absence of O_2 in the feed (at 500 °C, 50 mg catalyst, and a reaction feed consisting of NO (1%) in He (60 mL/min total flow rate), i.e. a WHSV of 0.95 g/$g_{catalyst}$/h).[15] Major efforts are currently focused on improving the tolerance of the catalysts to coexisting gases (e.g. O_2, CO_2, SO_2).[11,13]

In this context, the present work aims at investigating for the first time the potential of $H_3PW_{12}O_{40}$, the most widely used Keggin HPA, in the direct decomposition of continuously fed NO_x, at 380 °C, namely the temperature above which the HPA starts to irreversibly lose its protons.[18] An original methodology is proposed here to favor the NO_x decomposition process based on results recently reported in the literature for the HPAs system. On the one hand, NO was concluded to enter only the bulk of hydrated HPAs, and provided that O_2 (1-5%) was contained in the feed.[19,20] On the other hand, in the gas phase condensation of methanol into dimethylether (DME) at 150 °C,[21,22] methanol was also found to be unable to enter the bulk of anhydrous HPA crystals at the reaction temperature, unless the HPA had been previously exposed to methanol at lower temperature (RT). This was ascribed to a strong enough surface pre-adsorption at RT, followed by diffusion into the bulk upon heating to 150 °C which

finally further enabled the bulk of the HPA to become accessible also to methanol from the reaction feed at 150 °C. This low-temperature methanol pre-exposure led to a 5 times higher methanol-to-DME conversion than observed over classically activated HPA. On this basis, in the present work, the NO_x decomposition reaction will be investigated without or with pre-exposure of the hydrated HPA sample to the NO-O_2 feed at RT. Through a combination of essentially gas-infrared analysis, mass spectrometry and *in situ* diffuse reflectance infrared Fourier-transform spectroscopy under various reaction conditions, the present work sheds light on the activity of $H_3PW_{12}O_{40}$ in the aforementioned NO_x decomposition process, the nature of its active species in that process, and the sources of its deactivation. Thereby it unprecedentedly places HPAs into the category of materials to be considered on the way towards efficient formulations for direct NO_x decomposition.

2. Experimental section

2.1. Sample preparation

$H_3PW_{12}O_{40}$ (hereafter HPW12) was purchased from Sigma-Aldrich in the form of $H_3PW_{12}O_{40}.xH_2O$ (reagent grade). The powder was placed overnight under vacuum (< 5000 Pa) at room temperature (RT) in order to evacuate as much physisorbed water as possible. As revealed by a subsequent thermogravimetric analysis, the evacuated HPA contained 6 molecules of structural water per HPW12 unit ($x = 6$, thermogram not shown). Before experiments, the HPW12.6H_2O powder was sieved below 125 µm.

2.2. Direct NO_x decomposition experiments

Direct NO_x decomposition experiments were carried out in a U-shape quartz reactor (15 mm i.d.) at atmospheric pressure. The samples (2.5 g, < 125 µm) were held on plugs of quartz wool, and the temperature was controlled by a temperature controller (Eurotherm 2408) using a K type thermocouple. The reaction feed consisted of NO (~ 2000 ppm) in Ar(13%)/He, with or without O_2 (5%, if present), depending on the steps of the experiments (ppm and % referring to volume). The constitutive gases were fed from independent gas cylinders (Air Liquide), through independent mass flow controllers (Brooks 5850TR). The total flow rate was 50 mL$_{NTP}$/min. The reactor inlet and outlet gas flows were analyzed with a gas-infrared (IR) analyzer (MKS MultiGas 2030), which allowed simultaneously detecting H_2O, NO, NO_2 and N_2O (with 1 record every sec), as well as with a Pfeiffer Vacuum OmniStar mass spectrometer (MS) to qualitatively monitor the formation of N_2 using Ar as an internal standard (with 1 record every 6-6.5 sec), and occasionally with an Agilent CP490 micro-gas chromatograph (µ-GC) to quantify N_2 (with 1 injection every 3.5 min). As the concentration of N_2O remained below 0.6 ppm in all experiments, it is not reported in the results and discussion section.

In a first experiment, the sample – hereafter referred to as "N-HPW12" sample (N standing for non-NO_x-pre-saturated) – was heated from RT to 380 °C, the reaction temperature of interest in this work, at 10 °C/min under He (50 mL_{NTP}/min). Once H_2O was no longer detected by the gas-IR analyzer, i.e. once all of the structural water had been released (Figure S1a in the Supplementary Information), the sample was exposed to the O_2-free reaction feed (~ 2000 ppm NO – 13% Ar/He) for 60 minutes. Then, the sample was kept under static NO-Ar/He for 2 hours. Meanwhile, O_2 was introduced into the NO-Ar/He feed. 2 hours was the time needed to achieve stable IR and MS traces. Finally, the sample was exposed overnight to the O_2-containing reaction feed (~ 2000 ppm NO – 5% O_2 – 13% Ar/He).

In a second experiment, the sample was first pre-exposed to the O_2-containing reaction feed at RT for 4.5 days until the NO_x (NO + NO_2) inlet readout was equivalent to the NO_x outlet readout. The resulting "P-HPW12" sample (P standing for NO_x-pre-saturated) was then heated from RT to 380 °C at 3 °C/min under Ar(8%)/He (50 mL_{NTP}/min). The temperature ramp was slower than that used for N-HPW12 to avoid decomposing the NO_x species, that might have been retained by the sample at RT, into N_2 before reaching 380 °C.[23] At 380 °C, once H_2O was no longer detected by the gas-IR analyzer, i.e. once no structural water was released anymore (Figure S1b), the sample was first exposed overnight to the O_2-free reaction feed (~ 2000 ppm NO – 13% Ar/He), before being flushed under He (50 mL_{NTP}/min) for 10 hours, and then being exposed once again to the same O_2-free reaction feed for 3 hours. Finally, after having been kept under static NO-Ar/He for 2 hours (for the same reasons as N-HPW12 in the first experiment), the sample was exposed overnight to the O_2-containing reaction feed (~ 2000 ppm NO – 5% O_2 – 13% Ar/He). As explained in the introduction section, pre-exposing the hydrated HPW12 sample to the O_2-containing NO feed at RT before dehydration (upon heating to 380 °C) was likely to enable the protons located in the bulk of its crystals to participate in the direct decomposition of NO_x from the feed at 380 °C.

The exposure of the samples to the O_2-containing reaction feed at 380 °C in the above described experiments was repeated over fresh N-HPW12 and P-HPW12 samples (not having been beforehand exposed to the O_2-free reaction feed at 380 °C). As the results were essentially the same as those obtained in the above described experiments, they are not reported in the results and discussion section.

As references for these experiments, two blank experiments were also carried out, under the same reaction conditions as those aforementioned, but with only quartz wool in the reactor. The first reference experiment was performed with the O_2-free reaction feed, whereas the second one was performed with the O_2(5%)-containing feed.

2.3. In situ diffuse reflectance Fourier-transform infrared (DRIFT) spectroscopy

In order to gain further insight into the behavior of N-HPW12 and P-HPW12 under the O_2-free and O_2(5%)-containing reaction feeds, *in situ* diffuse reflectance infrared Fourier-transform (DRIFT) spectroscopy was carried out on similarly pre-treated samples under reaction conditions very close to those described in section 2.2, using a Bruker TENSOR II spectrometer. The reaction feed consisted of

NO (~ 2000 ppm) in Ar(40%)/He (50 mL$_{NTP}$/min total flow rate), with or without O$_2$ (5%, if present), depending on the steps of the experiments. It was prepared using the gas distribution setup described in section 2.2, and then conducted through a Harrick heatable variable atmosphere cell (HVAC) equipped with two ZnSe windows and one quartz window, in which the sample holder was filled with powder of the HPW12 samples (< 125 µm). The content of Ar in the feed was higher than that used in the experiments described in section 2.2, for thermal conductivity reasons. The samples, referred to as N-HPW12 and P-HPW12, were both heated from RT to 380 °C at 3 °C/min under Ar(40%)/He (50 mL$_{NTP}$/min). The pre-exposure of P-HPW12 to NO$_x$ at RT was carried out in the IR cell, under the O$_2$-containing reaction feed. At 380 °C, the first exposure to NO$_x$ was performed once the IR absorption band at 1740 cm^{-1}, characteristic of the structural water within HPW12,[19] had disappeared from the DRIFT spectrum (Figure S2, spectrum c *vs.* spectrum a of N-HPW12 at 380 °C *vs.* RT, and spectrum d *vs.* spectrum b of P-HPW12 at 380 °C *vs.* RT).[19] *In situ* DRIFT spectra of the samples were recorded using 128 scans and a resolution of 4 cm^{-1}. A reference spectrum was recorded with KBr (Fluka, purity > 99.5%) under the same operating (Ar(40%)/He (50 mL$_{NTP}$/min)) and temperature conditions. The absolute spectra are reported in log 1/R with R = I$_{sample}$ / I$_{KBr}$. The difference DRIFT spectra are reported in log 1/R' with the relative reflectance R' = I$_{sample}$ / I$_{(reference \ sample)}$.[24] Spectra processing was done using the Thermo Scientific OMNIC 9 software.

3. Results and Discussion

In the two blank experiments – one under the O$_2$-free reaction feed, the other one under the O$_2$(5%)-containing one – the MS-recorded mass to charge (m/z) ratio 28 associated with N$_2$ normalized by the m/z 40 one associated with Ar, as well as the sum of the NO and NO$_2$ concentrations recorded by the gas-IR analyzer, remained essentially unchanged after flowing the reaction feed through the reactor at 380 °C. This indicates that there was no NO$_x$ decomposition to N$_2$ occurring in the absence of HPW12 sample, and that there was no unwanted source of N$_2$ formation associated with the reactor. As an example, the N$_2$/Ar trace and the NO+NO$_2$ concentrations recorded in the presence of O$_2$ in the feed are shown in Figure S3. Due to the presence of O$_2$ in the feed, the NO and NO$_2$ concentrations were impacted by the non-catalytic conversion of NO to NO$_2$, to a larger extent after the feed had flown through the reactor at 380 °C. This needs to be kept in mind for discussing the results obtained over the HPW12 samples in the following subsections.

3.1. Activity of non-NO$_x$-pre-saturated H$_3$PW$_{12}$O$_{40}$ (N-HPW12) in the direct decomposition of NO$_x$

3.1.1. In the absence of O$_2$ in the reaction feed

Figure 1 shows the NO and NO$_2$ concentrations recorded by the gas-IR analyzer (panel a) as well as the MS-recorded mass to charge (m/z) ratios 28 and 32 associated with N$_2$ and O$_2$, respectively,

normalized by the m/z 40 one associated with Ar (panels b and c, respectively) as a function of time on stream in the NO$_x$ decomposition experiment carried out with the N-HPW12 sample at 380 °C, in the absence of O$_2$ in the reaction feed. The sample was previously heated from RT to 380 °C at 10 °C/min under He (50 mL$_{NTP}$/min). The NO$_x$ decomposition experiment was launched at 380 °C once no structural water was released from the sample anymore, as monitored with the gas-IR analyzer (Figure S1a). The reaction feed consisted of NO (~ 2000 ppm) in Ar(13%)/He (50 mL$_{NTP}$/min total flow rate). In period (i) of Figure 1, the reaction feed was analyzed for 5 min (time -5 to 0 min) without being contacted with the sample (upon flowing exclusively through lines at RT). In period (ii) of Figure 1, the reaction feed was continuously contacted with the sample at 380 °C, and the outlet gas flow was analyzed over time on stream.
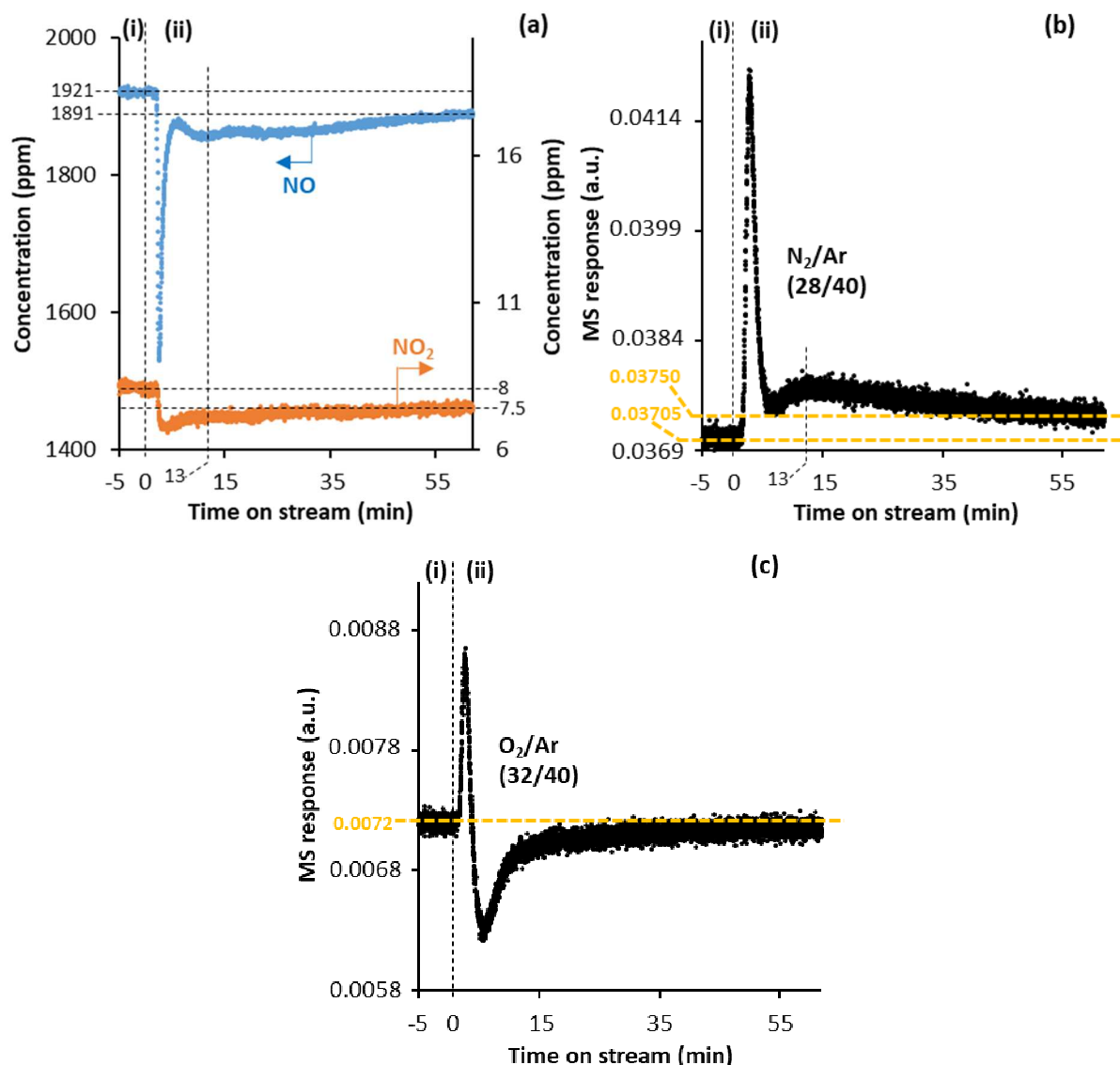
Figure 1. NO and NO$_2$ concentrations recorded by the MKS MultiGas 2030 IR analyzer (a) and mass to charge (m/z) ratios 28 and 32 associated with N$_2$ and O$_2$, respectively, normalized by the m/z 40 one associated with Ar recorded by the MS (b-c) as a function of time on stream in the NO$_x$ decomposition experiment with N-HPW12 (2.5 g, < 125 µm, N standing for non-NO$_x$-pre-saturated) at 380 °C and a reaction feed consisting of NO (~ 2000 ppm) in Ar(13%)/He (50 mL$_{NTP}$/min). In (i), the reaction feed was analyzed without being contacted with the sample (upon flowing exclusively through lines at RT). In (ii), the reaction feed was continuously contacted with the sample at 380 °C, and the outlet gas flow was analyzed over time on stream. N-HPW12 was previously heated from RT to 380 °C at 10 °C/min under He (50 mL$_{NTP}$/min).

As measured by the gas-IR analyzer, the reaction feed contained 1921 ppm of NO and 8 ppm of NO$_2$ (Figure 1a, period (i)). Upon starting period (ii) (time = 0 min), the concentration of NO in the outlet gas flow (Figure 1a) dropped from 1921 to 1520 ppm within the first 2 min on stream, and then immediately increased until reaching 1874 ppm at 6 min on stream. This initial peak of apparent NO consumption is attributed to the purge of the dead volume of the reactor, filled with He in period (i), upon introduction of the reaction feed. Afterwards, the recorded NO concentration evolved as a function of adsorption/reaction phenomena over the N-HPW12 sample. The concentration of NO first decreased from 1874 ppm at 6 min on stream to 1859 ppm at 13 min on stream. Then, it slowly increased until reaching 1891 ppm at the end of period (ii). The concentration of NO$_2$ remained between 6.5 and 7.5

7

ppm over the whole period (ii). The fact that it was lower in period (ii) than in period (i) suggests that NO_2 was partly adsorbed and/or converted on N-HPW12. The possible impact of the latter process on the interaction of N-HPW12 with NO will be discussed in the next sections (3.1.2, and 3.2 to 3.4).

The evolution of the N_2/Ar trace recorded by the MS (Figure 1b) inversely follows that of the NO concentration (Figure 1a). In period (ii), following its initial peak attributed to the evacuation of traces of air from the dead volume of the reactor, the N_2/Ar trace first increased from 5 to 13 min on stream, and then slowly decreased until the end of the experiment, reaching a final signal being however above that measured in period (i). According to a calibration based on μ-GC measurements (the error associated to which is estimated to be about 1.6%), the difference between the final N_2/Ar signals in periods (ii) and (i) corresponds to about 18 ppm of N_2 produced, thus close to half the concentration of NO (30 ppm) missing in the outlet gas flow as compared to the feed (Figure 1a, end of period (ii) *vs.* period (i)). These results demonstrate, to our knowledge for the first time, that direct decomposition of NO into N_2 (2 NO → N_2 + O_2) occurs over HPW12 under continuous NO feeding at 380 °C (with a rate of 5.9 x 10^{-16} μmol/g_{HPW12}/s after 60 min on stream, with 2.5 g of HPW12 and a reaction feed consisting of NO (~ 2000 ppm) in Ar(13%)/He (50 mL_{NTP}/min), i.e. a WHSV of 3.2 x 10^{-3} g/g_{HPW12}/h). The evolution of this NO decomposition activity with time on stream is further discussed in section 3.4.

In period (ii) of Figure 1, the initial peak observed for the N_2/Ar trace (Figure 1b), which was attributed earlier to the evacuation of traces of air from the dead volume of the reactor, was also observed for the O_2/Ar trace (Figure 1c). Afterwards, however, while the N_2/Ar trace increased from 5 to 13 min on stream, and then slowly decreased until the end of the experiment, reaching a final signal being however above that measured in period (i) (Figure 1b), the O_2/Ar trace first decreased until 8 min on stream, and then increased until the end of the experiment (rapidly from 8 to 15 min on stream, then more slowly from 15 min on stream to the end), reaching a final signal being slightly below that measured in period (i) (Figure 1c). This comparison suggests that, while N_2 was produced over N-HPW12 by NO decomposition, traces of O_2 contained in the NO feed and/or O_2 produced together with N_2 over N-HPW12 by NO decomposition were getting adsorbed/not getting desorbed onto/from the Keggin units. The link between the latter phenomenon and the decreasing activity of N-HPW12 in Figure 1a-b will be made in section 3.4.2. Non-catalytic NO oxidation into NO_2 with traces of O_2 contained in the NO feed or O_2 produced from the NO decomposition process over N-HPW12 must be negligible, as the concentration of NO converted (30 ppm at the end of the experiment, Figure 1a) was close to that expected from the concentration of N_2 produced (18 ppm at the end of the experiment, Figure 1b).

3.1.2. In the presence of O_2 in the reaction feed

Figure 2 shows the NO and NO_2 concentrations recorded by the gas-IR analyzer in the NO_x decomposition experiment over N-HPW12 at 380 °C in the presence of O_2 in the reaction feed (with panels a and b showing the same data over two different time scales, for the sake of clarity). In period

(i), the reaction feed consisting of NO (~ 2000 ppm) in O_2(5%)-Ar(13%)/He (50 mL$_{NTP}$/min) was analyzed for 5 min without being contacted with the sample (upon flowing exclusively through lines at RT). It was found to contain 1770 ppm of NO and 194 ppm of NO_2 (Figure 2a). Meanwhile, the sample was kept under static NO-Ar/He (from the O_2-free reaction feed used in the preceding step of the experiment, Figure 1). In period (ii), the reaction feed was continuously contacted with the sample at 380 °C, and the outlet gas flow was analyzed over time on stream.
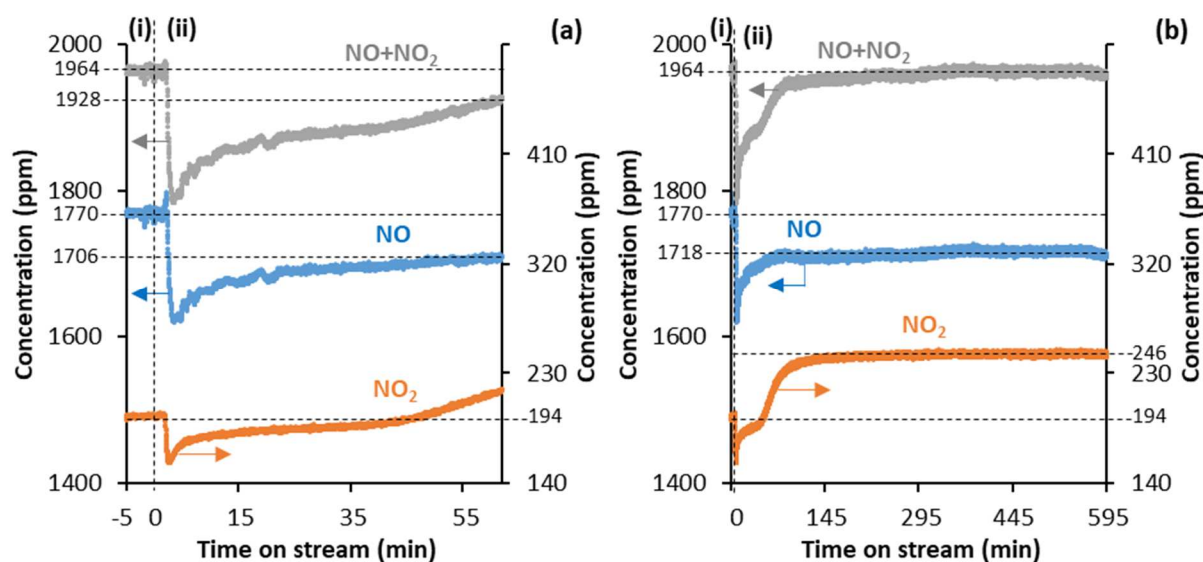

Figure 2. NO and NO_2 concentrations recorded by the MKS MultiGas 2030 IR analyzer as a function of time on stream in the NO_x decomposition experiment with N-HPW12 (2.5 g, < 125 µm, N standing for non-NO_x-pre-saturated) at 380 °C and a reaction feed consisting of NO (~ 2000 ppm) in O_2(5%)-Ar(13%)/He (50 mL$_{NTP}$/min). In (b), for the sake of clarity, the same data as in (a) is shown over a longer time scale. In (i), the reaction feed was analyzed without being contacted with the sample (upon flowing exclusively through lines at RT). In (ii), the reaction feed was continuously contacted with the sample at 380 °C, and the outlet gas flow was analyzed over time on stream. N-HPW12 was previously heated from RT to 380 °C at 10 °C/min under He (50 mL$_{NTP}$/min).

The total NO_x concentration in the outlet gas flow in period (ii) remained lower than that in the feed in period (i) for about 300 min on stream. Given that N_2/Ar trace remained essentially unchanged after contacting the reaction feed with the sample (not shown), as also reported for the blank experiment over quartz wool (Figure S3b-c), NO_x species did not decompose into N_2, but were retained by the N-HPW12 sample in these first 300 min on stream (Figure 2). The NO_x species retained by the sample consisted mostly of NO_2, as indicated by the comparison of the concentrations of NO and NO_2 in the first 300 min on stream with those after 300 min on stream (Figure 2b), once the total NO_x concentration had finally reached the same level as in the feed (no NO_x species were retained anymore by the N-HPW12 sample). In the latter period, after 300 min on stream, the final NO/(NO+NO_2) and NO_2/(NO+NO_2) concentration ratios (1718/1964 = 0.875 and 246/1964 = 0.125, respectively, as measured in several repeat experiments) were slightly higher and lower, respectively, than the reference ratios observed over quartz wool at 380 °C (1675/1947 = 0.86 and 272/1947 = 0.14, respectively, Figure S3a), with the reference ratios being dictated by the non-catalytic oxidation of NO to NO_2. This suggests that N-HPW12 catalyzed the conversion of some NO_2 back to NO (whereas at RT, N-HPW12 was found to catalyze

9

the oxidation of NO, Figure 3). Indeed, at 380 °C, even if their Keggin structure is maintained,[18] the heteropolyanions may be deficient in structural oxygen atoms, and therefore may act as reducing agents towards NO_2. Actually, the filling of their O vacancies along with the reduction of NO_2 might explain the inactivity of N-HPW12 in the direct decomposition of NO_x in the present experiment, whereas this sample was found to be active in this reaction in the absence of O_2 in the feed (Figure 1). In collaboration with the protons known to activate NO and NO_2 to form NOH^+ and HNO_2^+ species, respectively,[9,23] the lacunary heteropolyanions might be the reductants required to finally decompose NO into N_2. A direct filling of the O vacancies by O_2 might then also contribute to the deactivation of N-HPW12, together with a possible poisoning of the protons by NO_2 to form stable HNO_2^+ species preventing NO from being activated. The deactivation of N-HPW12 after exposure to the O_2-containing reaction feed at 380 °C was found to be irreversible as no NO_x decomposition could be recorded when removing O_2 from the reaction feed (not shown).

3.2. Pre-saturation of $H_3PW_{12}O_{40}$ (HPW12) with NO_x species to yield the P-HPW12 sample

In the second NO_x decomposition experiment performed in the present work, $HPW12.6H_2O$ was first exposed to NO (~ 2000 ppm) in $O_2(5\%)$-Ar(13%)/He (50 mL_{NTP}/min) at RT before being heated under Ar(8%)/He (50 mL_{NTP}/min) to the reaction temperature 380 °C (3 °C/min). The sample obtained at the end of the pre-exposure step at RT is labelled as "P-HPW12" (P standing for NO_x-pre-saturated). The NO and NO_2 concentrations recorded by the gas-IR analyzer during the NO_x-pre-exposure step are shown in Figure 3 (with panels a and b showing the same data over two different time scales, for the sake of clarity). In period (i), the NO-O_2 feed was analyzed without being contacted with the sample. It was found to contain 1732 ppm of NO and 177 ppm of NO_2 (Figure 3a), due to the non-catalytic conversion of NO to NO_2 in the stainless-steel feeding lines. In period (ii), the feed was contacted with the sample, and the outlet gas flow was analyzed over time on stream.
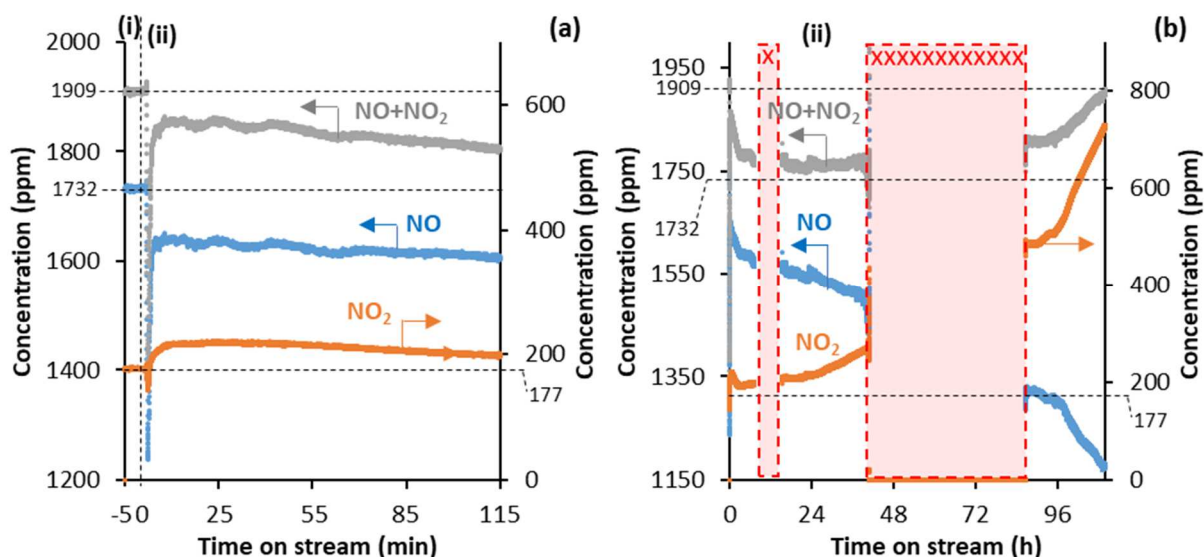
Figure 3. NO and NO$_2$ concentrations recorded by the MKS MultiGas 2030 IR analyzer as a function of time on stream in the pre-exposure of HPW12 (2.5 g, < 125 µm) to a 50 mL$_{NTP}$/min feed of NO (~ 2000 ppm) in O$_2$(5%)-Ar(13%)/He at RT, to yield the P-HPW12 sample. In (i), the feed was analyzed without being contacted with the sample. In (ii), the feed was contacted with the sample, and the outlet gas flow was analyzed over time on stream. (b) shows the same traces as (a), but over a longer time scale. The periods marked with crosses (xxx) correspond to night and/or weekend periods in which the cryo-detector of the IR analyzer could not be filled with liquid N$_2$.

The sum of the NO and NO$_2$ concentrations remained below its initial level of period (i) for 4.5 days on stream (Figure 3b). The missing NO$_x$ (NO+NO$_2$) concentration in the outlet gas flow was integrated over the whole 4.5 days on stream, by roughly interpolating the NO$_x$ concentration in the periods of missing data (i.e. night and weekend periods during which the cryo-detector of the analyzer could not be filled with liquid N$_2$). This yielded a value of 0.0020 mol of NO$_x$ retained by the sample, that corresponds to 81% of the total amount of protons (0.0024 mol) contained in the sample (2.5 g). Given that surface protons represent only 4% of the total number of protons of HPW12,[22] the amount of NO$_x$ stored in the present experiment as NOH$^+$ or HNO$_2^+$ species[19,20] (81% of the protons) demonstrates that NO$_x$ had largely entered the bulk of the P-HPW12 crystals, which confirms the great potential of Keggin HPAs as NO$_x$ absorber materials, as pointed out in the introduction section.[9] Thereby, the structural water was progressively evacuated from the P-HPW12 crystals during the pre-exposure to NO$_x$ at RT (Figure S4). This explains why, upon heating the P-HPW12 sample afterwards from RT to 380 °C (3 °C/min) under Ar(8%)/He (50 mL$_{NTP}$/min), only 25% of the total amount of structural water theoretically contained in HPW12.6H$_2$O (2.5 g) was released (Figure S1b). It can therefore be concluded that the pre-exposure of the HPW12 sample to NO$_x$ at RT had already evacuated 75% of the structural water.

At the very end of period (ii), when the total NO$_x$ concentration in the outlet gas flow was equal to that in the feed (1909 ppm in period (i)), indicating that NO$_x$ absorption by P-HPW12 was completed, the concentrations of NO and NO$_2$ were significantly lower and higher, respectively, than those in the feed (1174 *vs.* 1732 ppm and 736 *vs.* 177 ppm, respectively). This is attributed to the catalytic oxidation of NO into NO$_2$ at the surface of P-HPW12.[19] The total amounts of NO and NO$_2$ retained by the sample

can be assumed to be similar, as upon heating the P-HPW12 sample afterwards from RT to 380 °C (3 °C/min) under Ar(8%)/He (50 mL$_{NTP}$/min), nearly the same amounts of NO and NO$_2$ were released (7.42 x 10^{-5} mol of NO *vs.* 7.61 x 10^{-5} mol of NO$_2$, Figure S5a). Notice that the total amount of NO$_x$ released (1.503 x 10^{-4} mol) upon heating the P-HPW12 sample from RT to 380 °C corresponds to only 7.5% of the 0.0020 mol of NO$_x$ initially retained at RT. Some N$_2$ was also detected upon heating the P-HPW12 sample from RT to 380 °C (Figure S5b), but as the temperature ramp used was as slow as 3 °C/min, according to earlier literature reports, the corresponding N$_2$ amount remained limited to about 5% of the pre-absorbed NO$_x$ species.[9,23] Once the temperature was stabilized at 380 °C, no N$_2$ was formed anymore, showing that the pre-absorbed NO$_x$ species were unable to decompose at a constant temperature of 380 °C under inert atmosphere. Overall, it can be concluded that the sample still contained the majority of its pre-absorbed NO$_x$ species at the start of the experiment performed with continuously fed NO$_x$ at 380 °C.

3.3. Activity of NO$_x$-pre-saturated H$_3$PW$_{12}$O$_{40}$ (P-HPW12) in the direct decomposition of NO$_x$

3.3.1. In the absence of O$_2$ in the reaction feed – Elucidating the deactivating impact of NO$_2$ on the activity of HPW12

Figure 4a shows the NO and NO$_2$ concentrations recorded by the gas-IR analyzer as a function of time on stream in the NO$_x$ decomposition experiment over the P-HPW12 sample at 380 °C, in the absence of O$_2$ in the reaction feed. In period (i), the reaction feed – NO (~ 2000 ppm) in Ar(13%)/He – was analyzed for 5 min without being contacted with the sample (upon flowing exclusively through lines at RT). It was found to contain 1919 ppm of NO and 7 ppm of NO$_2$. Meanwhile, the sample was kept under static Ar/He, the atmosphere under which the sample was previously heated from RT to 380 °C. In period (ii), the reaction feed was continuously contacted with the sample at 380 °C, and the outlet gas flow was analyzed over time on stream. Figure S6 shows the same concentrations over a longer time scale (600 min).
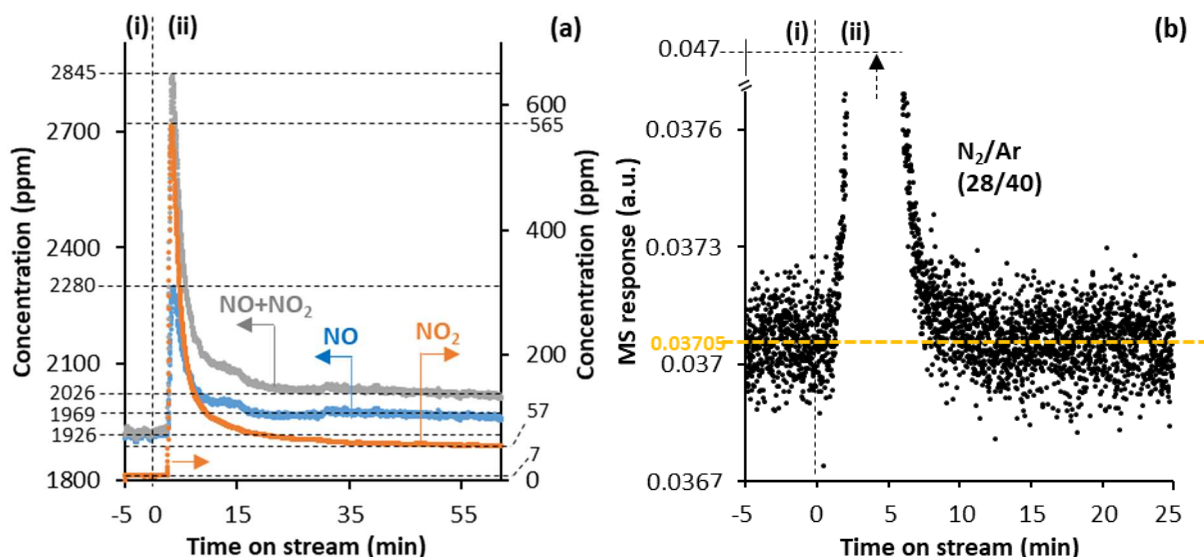
Figure 4. NO and NO$_2$ concentrations recorded by the MKS MultiGas 2030 IR analyzer (a) and mass to charge (m/z) ratio 28 associated with N$_2$ normalized by the m/z 40 one associated with Ar recorded by the MS (b) *vs.* time on stream in the NO$_x$ decomposition experiment with P-HPW12 (2.5 g, < 125 µm, P standing for NO$_x$-pre-saturated) at 380 °C and a reaction feed consisting of NO (~ 2000 ppm) in Ar(13%)/He (50 mL$_{NTP}$/min). In (i), the reaction feed was analyzed without being contacted with the sample (upon flowing exclusively through lines at RT). In (ii), the reaction feed was continuously contacted with the sample at 380 °C, and the outlet gas flow was analyzed over time on stream. The N$_2$/Ar peak at around 5 min on stream has no analytical interest here. It is attributed to the release of air trapped in the valve that served for contacting the reaction feed with the sample. Its upper intensity was cut from the graph, as indicated by the rising arrow. The P-HPW12 sample was previously heated from RT to 380 °C at 3 °C/min under Ar(8%)/He (50 mL$_{NTP}$/min).

Within the first 3 min of period (ii), the concentrations of NO and NO$_2$ in the outlet gas flow rose up quickly to 2280 and 565 ppm, respectively, whereas they were found to drop in the equivalent experiment over N-HPW12 (Figure 1). This indicates that, during the preceding period (i), the static Ar/He atmosphere had been progressively enriched in NO and NO$_2$ being released from the sample, until it was evacuated along with the introduction of the reaction feed. Then, following this initial NO$_x$ peak in period (ii), both the NO and NO$_2$ concentrations decreased until reaching, at about 35 min on stream, stable levels of 1969 and 57 ppm, respectively. These concentrations were both 50 ppm higher than those in the feed recorded in period (i), indicating that the sample was continuously releasing 50 ppm of both NO and NO$_2$, namely 4.4 times less NO and NO$_2$ than released under Ar(8%)/He right before switching to period (i) (Figure S5a, 219 ppm of both NO and NO$_2$ released at 184 min on stream). Thus, under reaction conditions, the NO feed essentially prevented the sample from releasing its pre-absorbed NO$_x$ species. However, unlike in the experiment carried out over N-HPW12 in the absence of O$_2$ in the feed (Figure 1), NO from the feed was not decomposed to N$_2$, as the N$_2$/Ar MS trace remained essentially unchanged from period (i) to period (ii) (Figure 4b). The absence of NO$_x$ decomposition activity of P-HPW12, whereas N-HPW12 was active under the same O$_2$-free conditions, can only be attributed to the presence and/or the release of NO$_2$ in the/out of the bulk of its crystals, which is the only significant difference between the experiments carried out on these two samples in the absence of O$_2$ in the feed. As in the experiment performed over N-HPW12 in the presence of O$_2$ in the feed, NO$_2$ might have filled the O vacancies of the heteropolyanions, preventing them from playing their possible

13

role as NO reductants, or might have poisoned the protons to form unreactive HNO_2^+ species, eventually preventing NO from being activated.

Following this first NO_x decomposition experiment over P-HPW12 at 380 °C in the absence of O_2 in the feed (Figure 4), the sample was purged under He (50 mL_{NTP}/min) at 380 °C for 10 hours, before being exposed a second time to the same O_2-free reaction feed for 3 hours (Figure S7). During this second exposure to the O_2-free reaction feed, the concentrations of NO and NO_2 continuously released from the sample were lower than in the first reaction step (Figure S7 *vs.* Figure 4). From about 50 min on stream, once the concentrations had stabilized, only 20 ppm of both NO and NO_2 were released (whereas 50 ppm were released in the first experiment, Figure 4). This shows that the amount of NO_x species released in the feed in the course of the experiment depends on the amount of NO_x species stored in the sample, the latter amount being lower after the purge step during which a part of the pre-absorbed NO_x species was released (not shown). As in the first experiment, the NO_x (fed and pre-absorbed) were not found to decompose into N_2 (not shown).

3.3.2. In the presence of O_2 in the reaction feed – Elucidating the positive impact of O_2 on the activity of HPW12

The P-HPW12 sample already used in the two latter experiments (section 3.3.1) was finally submitted to a NO_x decomposition experiment at 380 °C in the presence of O_2 in the reaction feed. The NO and NO_2 concentrations recorded by the gas-IR analyzer as a function of time on stream are shown in Figure 5a-b (with panels a and b showing the same data over two different time scales, for the sake of clarity), whereas the N_2/Ar trace recorded by the MS is shown in Figure 5c. In period (i), the reaction feed consisting of NO (~ 2000 ppm) in O_2(5%)-Ar(13%)/He (50 mL_{NTP}/min) was analyzed for 5 min without being contacted with the sample (upon flowing exclusively through lines at RT). It was found to contain 1736 ppm of NO and 181 ppm of NO_2. Meanwhile, the sample was kept under static NO-Ar/He (from the O_2-free reaction feed used in the preceding step of the experiment, Figure 4). In period (ii), the reaction feed was continuously contacted with the sample at 380 °C, and the outlet gas flow was analyzed over time on stream.

In period (ii) of Figure 5a-b, the total NO_x concentration in the outlet gas flow first decreased, and then immediately increased to slightly above its level in the feed. Then, it decreased again up to about 20 min on stream, before remaining below its level in the feed until the end of the experiment. Thus, unlike in the absence of O_2 in the feed (Figure 4a), NO_x from the feed were retained by the P-HPW12 sample in the presence of O_2 in the feed. The fact that the NO, NO_2 and total NO_x concentrations remained essentially constant from about 20 to 100 min on stream (Figure 5a-b) indicates that NO_x were retained not only at the surface but also in the bulk of P-HPW12. Indeed, in the pre-saturation of P-HPW12 with NO_x at RT, the NO_x concentration was also constant for a significant period of time (Figure 3b), and this was demonstrated in section 3.2 to arise from bulk absorption, probably due to diffusion limitations in-between the constitutive HPW12 units.[22] In the present experiment, during the last 200 min on stream

(Figure 5b), the total NO_x concentration was relatively close to that in the feed (only 14 ppm lower, whereas it was 71 ppm lower at 100 min on stream), which means that the sample was still retaining only a limited amount of NO_x from the feed. By comparing the individual NO and NO_2 concentrations in that final period with those in the period from 20 to 100 min on stream (1670 *vs.* 1643 ppm of NO, and 233 *vs.* 207 ppm of NO_2), it can be concluded that, in the period from 20 to 100 min on stream, both NO and NO_2 were absorbed by the sample in similar proportions (27 ppm of NO absorbed per unit of time *vs.* 26 ppm of NO_2).
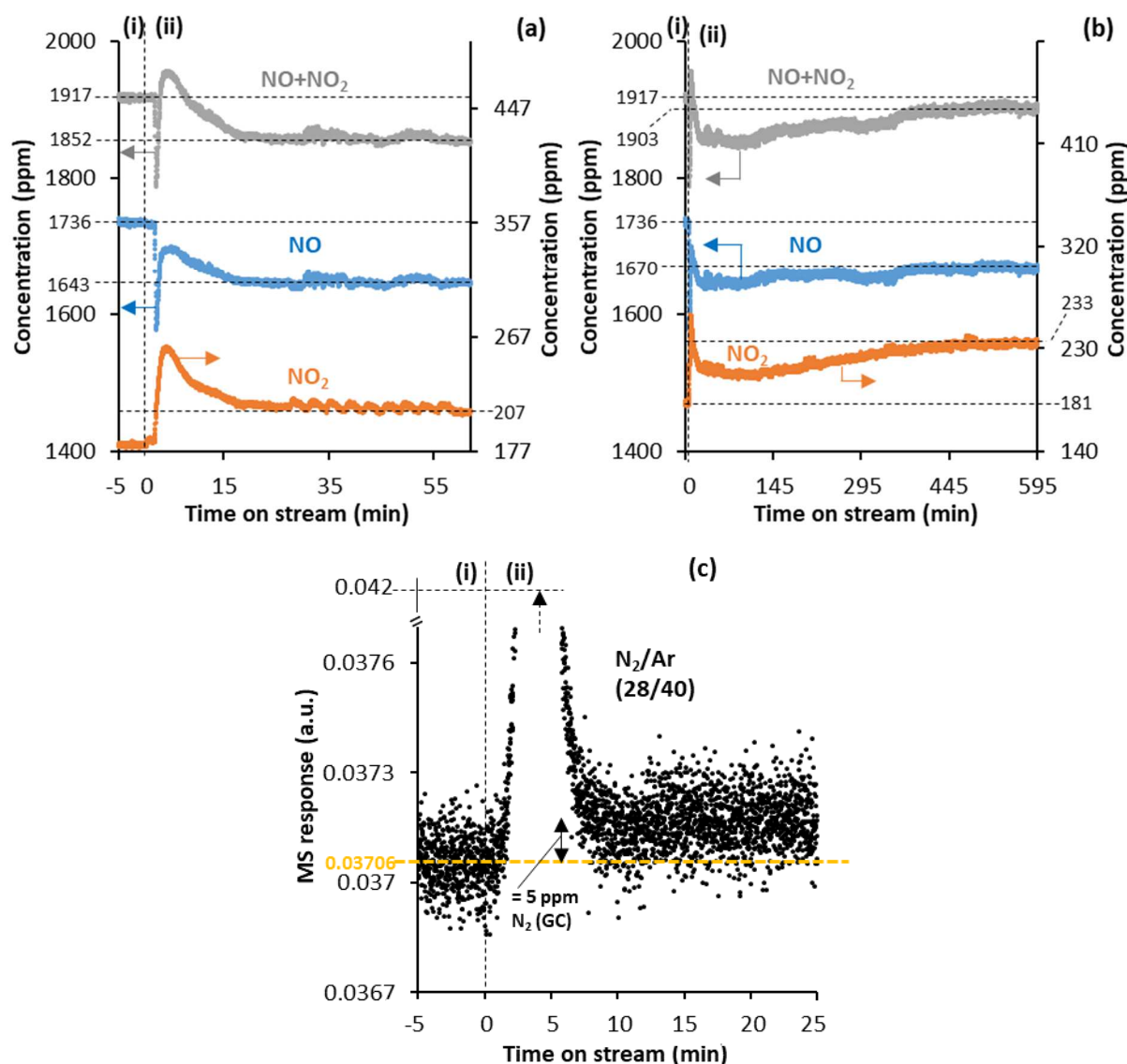

Figure 5. NO and NO_2 concentrations recorded by the MKS MultiGas 2030 IR analyzer (a-b) and mass to charge (m/z) ratio 28 associated with N_2 normalized by the m/z 40 one associated with Ar recorded by the MS (c) as a function of time on stream in the NO_x decomposition experiment with the P-HPW12 sample (2.5 g, < 125 µm, P standing for NO_x-pre-saturated) at 380 °C and a reaction feed consisting of NO (~ 2000 ppm) in O_2(5%)-Ar(13%)/He (50 mL_{NTP}/min). In (b), for the sake of clarity, the same data as in (a) is shown over a longer time scale. In (i), the reaction feed was analyzed without being contacted with the sample (upon flowing exclusively through lines at RT). In (ii), the reaction feed was continuously contacted with the sample at 380 °C, and the outlet gas flow was analyzed over time on stream. The N_2/Ar peak at around 5 min on stream has no analytical interest here. It is attributed to the release of air trapped in the valve that served for contacting the reaction feed with the sample. Its upper intensity was cut from the graph, as indicated by the rising arrow. This experiment with P-HPW12 was the third one over the same sample. The two first ones were carried out in the absence of O_2 in the feed (Figure 4 and Figure S7, respectively). The P-HPW12 sample was previously heated from RT to 380 °C at 3 °C/min under Ar(8%)/He (50 mL_{NTP}/min).

The fact that the presence of O_2 in the feed induced a diffusion of NO_2 into the bulk of P-HPW12 is attributed to the relatively high concentration of NO_2 in the feed under these conditions (181 ppm in Figure 5a-b *vs.* 7 ppm in Figure 4a, periods (i)). The fact that, at the same time, it also enabled the diffusion of NO into the bulk may be assigned to two possible origins. Firstly, NO might have been brought up into the bulk of HPW12 concomitantly with NO_2 via the formation of N_2O_3.[25] Secondly, O_2 might have reacted with NO at the surface of the crystals to form intermediate NO_x^{y-} adspecies being easily protonated by the protons located in the near-surface bulk of HPW12 (thereby regenerating O_2) and consequently leading to the absorption of NO into the bulk of HPW12.[19] Overall, the presence of O_2 in the feed appears to be required for NO to form a species that is able to diffuse into the bulk of HPW12.

The diffusion of NO_x into the bulk of P-HPW12 led to the decomposition of NO_x from the feed and/or of NO_x pre-absorbed in the bulk into N_2. Indeed, in period (ii) of Figure 5c, following its initial peak centered at around 5 min on stream, attributed to the evacuation of traces of air trapped in the 4-way valve used for contacting the reaction feed with the sample, the N_2/Ar trace stabilized at a higher level than that measured in period (i). As shown in Figure S8, the production of N_2 remained stable for about 200 min on stream, before decreasing to the level measured in period (i) within the next 300 min. According to μ-GC measurements (the error associated to which is estimated to be about 1.6%), about 5 ppm of N_2 were produced per unit of time in the first 200 min on stream, which corresponds to 10 ppm of NO_x decomposed per unit of time. From 200 to 500 min on stream, while the N_2/Ar signal was decreasing (Figure S8), the NO, NO_2, and total NO_x concentrations were increasing (Figure 5b). This shows that the deactivation of P-HPW12 was directly related to the decreasing capacity of its bulk to further incorporate NO_x species. To explain this finding, two non-exclusive hypotheses may be proposed. Firstly, once the NO_x from the feed were no longer able to react over the deactivated bulk HPW12 units, they accumulated inside the bulk until saturating it. In this hypothesis, the HPW12 units may have been deactivated following the two non-exclusive mechanisms proposed earlier in the present work: 1) the O vacancies in the heteropolyanions getting filled by O_2 and/or NO_2, and/or 2) the protons associated with the heteropolyanions getting poisoned by NO_2 as HNO_2^+ species. Secondly, once the NO_x species pre-absorbed in the bulk had all been consumed by the decomposition reaction with NO_x from the feed, the bulk was essentially emptied, and therefore no longer accessible.[21]

3.4. Comparison of the NO_x decomposition activities of N-HPW12 and P-HPW12

Table 1 qualitatively summarizes the activities observed over the N-HPW12 and P-HPW12 samples in the direct decomposition of continuously fed NO_x at 380 °C in the absence and in the presence of O_2 in the reaction feed. In section 3.4.1, the role of pre-absorbed NO_x species in the activity of P-HPW12 in the decomposition of NO_x from the O_2-containing reaction feed is discussed (by comparing the activities of N-HPW12 and P-HPW12 shown in Figure 2 *vs.* Figures 5 and S8, respectively). In section

3.4.2, the activity of N-HPW12 in the absence of O_2 in the reaction feed (Figure 1) is compared to that of P-HPW12 in the presence of O_2 in the reaction feed (Figures 5 and S8) in terms of NO conversion and stability over time on stream.

Table 1. Qualitative summary of the activities observed over the N-HPW12 and P-HPW12 samples (2.5 g, < 125 µm) in the direct decomposition of continuously fed NO_x at 380 °C in the absence and presence of O_2 (5%) in the reaction feed (Figures 1-2, 4-5 and S6 to S8). The reaction feed contained NO (~ 2000 ppm) in Ar(13%)/He (50 mL$_{NTP}$/min total flow rate). The N-HPW12 and P-HPW12 samples were previously heated from RT to 380 °C at 10 °C/min under He and at 3°C/min under Ar(8%)/He, respectively (50 mL$_{NTP}$/min). Unlike the N-HPW12 sample, the P-HPW12 sample was pre-saturated with NO_x at RT (N and P standing for non-NO_x-pre-saturated and NO_x-pre-saturated, respectively). "Min" are min of reaction, not including the 5 min in which the reaction feed was analyzed without being contacted with the sample, namely period (i) in Figures 1-2, 4-5 and S6 to S8.

Reaction feed	Concentration of NO_x decomposed into N_2	
	Over N-HPW12	Over P-HPW12
O_2-free	- Essentially decreasing in the 60 min considered - At 60 min, 30 ppm	0
O_2(5%)-containing	0	Stable at 10 ppm for 200 min before decreasing to 0 in 300 min

3.4.1. The positive impact of the pre-saturation of HPW12 with NO_x species on its NO_x decomposition activity in the presence of O_2 in the reaction feed, and the balance between positive and deactivating impacts of O_2

The second hypothesis proposed at the end of section 3.3.2 to account for the observed deactivation of P-HPW12, namely that a NO_x-emptied HPW12 bulk is no longer accessible to NO_x from the feed, arises from the fact that NO_x were essentially unable to enter the bulk of the N-HPW12 sample at 380 °C despite the presence of O_2 in the feed. This assumption is supported by the absence of plateau in the NO and NO_2 concentration traces when the total NO_x concentration was significantly below that in the feed (when NO_x were retained by the sample), i.e. in the first 100 min on stream (Figure 2). Within this period, NO_x were essentially adsorbed onto the surface of N-HPW12, with a higher rate than that observed in the case of P-HPW12 (Figure 2 *vs.* Figure 5), as the surface of the latter had been already partly covered with NO_x species during the pre-saturation step at RT (Figure 2 *vs.* Figure 5). Thus, the presence of pre-absorbed NO_x appears to be necessary for NO and NO_2 to enter the bulk of HPW12 crystals at 380 °C, unlike at RT (Figure 3). This suggests that, rather than depending on the temperature as a source of energy to overcome the activation barrier of bulk absorption, the ability of NO_x to enter the bulk depends on the temperature as a modulator of the balance between the strength of adsorption at the surface of the crystals and the activation energy required to enter the bulk. At 380 °C, the adsorption of NO_x at the surface of N-HPW12 must be weaker than at RT, whereas the activation energy to enter its bulk is likely higher, due to the absence of structural water which requires the NO_x to open the way in-between the bulk HPW12 units. This makes the diffusion of NO_x into the bulk more difficult, unless

the presence of pre-absorbed NO_x species has already made the diffusion pathway in-between the bulk HPW12 units accessible, as in the case of P-HPW12.

In summary, the different NO_x decomposition activities observed for the N-HPW12 and P-HPW12 samples at 380 °C in the presence of O_2 in the feed (Figures 2 and 5, respectively) resulted from a balance between the negative impact of O_2 and/or NO_2 deactivating the heteropolyanions and/or their associated protons, and the positive impact of O_2 and/or NO_2 initiating the diffusion of NO into the bulk of the HPW12 crystals. The latter positive impact took place to a noticeable extent only in the case of P-HPW12 (Figure 5), thanks to NO_x species pre-absorbed in the bulk of HPW12 having made the diffusion pathway in-between the HPW12 units accessible to the NO_x from the reaction feed. This explains that P-HPW12 exhibited a NO_x decomposition activity in the presence of O_2 in the reaction feed, whereas N-HPW12 was found to be inactive in this reaction under the same conditions.

3.4.2. Comparison of the NO_x decomposition activity of N-HPW12 in the absence of O_2 in the reaction feed to that of P-HPW12 in the presence of O_2 in the reaction feed

The balance between the negative and positive impacts of O_2 and/or NO_2 described in section 3.4.1 was, however, still not sufficiently favorable for P-HPW12 to reach a NO_x decomposition activity in the presence of O_2 in the reaction feed (Figure 5) as high as that recorded on N-HPW12 in the absence of O_2 in the reaction feed (Figure 1). At 60 min of reaction, 10 ppm of NO_x were decomposed over P-HPW12 in the presence of O_2 in the feed (Figures 5c and S8), whereas 30 ppm of NO_x were decomposed over N-HPW12 in the absence of O_2 (Figure 1). Nevertheless, P-HPW12 exhibited a stable NO_x decomposition activity for as long as 200 min, thanks to the increased fraction of accessible HPW12 units whose deactivation was likely limited by NO_x diffusion inside the bulk,[22] whereas N-HPW12 showed a continuously decreasing activity in the considered 60 min of reaction. Indeed, even in the absence of O_2 intentionally added into the feed, the latter still contained a few ppm of deactivating NO_2 and traces of O_2, as well as O_2 that was produced along with the decomposition of NO over N-HPW12, which might have also led to the progressive filling of the O vacancies in the HPW12 units and thus to the deactivation of the sample. Such a progressive filling of the O vacancies might explain the progressive increase of the O_2/Ar signal from 8 min on stream in Figure 1c (the Keggin units exhibiting less and less O vacancies to be filled as the decomposition reaction proceeded).

3.5. Identifying the active sites of HPW12 in the direct decomposition of NO_x, and possible origins of their deactivation

Figure 6 shows the *in situ* DRIFT difference spectra at steady state of N-HPW12 at 380 °C under a 50 mL_{NTP}/min feed of NO (~ 2000 ppm) in Ar(40%)/He which first contained no O_2 (spectrum 1, NO) and subsequently contained 5% of O_2 (spectrum 2, NO+O_2). For the sake of clarity, panels a and b show the same spectra in two different spectral regions. Both difference spectra were obtained by subtraction

of the last spectrum recorded at 380 °C under Ar(40%)/He before NO was added into the feed. N-HPW12 was previously heated from RT to 380 °C at 3 °C/min under Ar(40%)/He (50 mL_{NTP}/min).

Both difference spectra show a positive band at 2261 cm^{-1}, and a broad negative band centered at 3230 cm^{-1}. In the presence of O_2 in the feed (spectrum 2 in Figure 6), the area of these two bands is 4.8 and 1.3 times higher, respectively, than in the absence of O_2 in the feed (spectrum 1 in Figure 6). In earlier studies about the absorption of NO and/or NO_2 into the bulk of HPW12 at temperatures around 150 °C, the band at 2261 cm^{-1} was assigned to ν(N=O) stretches within both NOH^+ and HNO_2^+ species.[19,20] The negative band at 3230 cm^{-1} was neither shown nor commented in earlier literature studies. It is attributed here to the consumption of HPA protons upon NOH^+ and/or HNO_2^+ formation. The higher areas of the bands at 2261 and 3230 cm^{-1} in the presence of O_2 in the feed can be attributed to two non-exclusive origins. Firstly, it may result from the 26 times higher concentration of NO_2 in the O_2-containing feed (181 ppm *vs*. 7 ppm in Figures 5a-b and 4a, respectively), which led to an increase of the concentration of HNO_2^+ adspecies, that may have reached the near-surface bulk of the HPW12 crystals to a little extent.[25] Secondly, it may result from the formation of NOH^+ species in the near-surface bulk of HPW12, thanks to either NO_2 as a carrier or O_2 having reacted with NO at the surface to form intermediate NO_x^{y-} adspecies that are potentially required to initiate bulk absorption.[19]
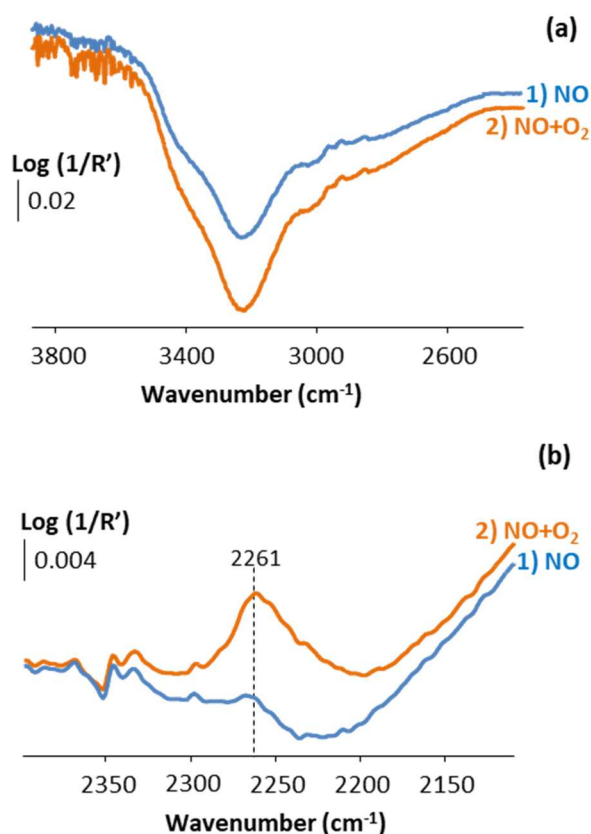
Figure 6. *In situ* DRIFT difference spectra of N-HPW12 (N standing for non-NO$_x$-pre-saturated) at 380 °C under a feed of NO (~ 2000 ppm) in Ar(40%)/He (50 mL$_{NTP}$/min) 1) since 12 h and 2) 8 h after adding O$_2$ (5%) into the feed, in the spectral regions of (a) structural O-H$^+$ stretches and (b) N=O stretches within NOH$^+$ and HNO$_2$$^+$ species. N-HPW12 was heated from RT to 380 °C at 3 °C/min under Ar(40%)/He (50 mL$_{NTP}$/min). Both difference spectra were obtained by subtraction of the last spectrum recorded at 380 °C under Ar(40%)/He before NO was added into the feed. Log (1/R') is expressed in arbitrary units, with the relative reflectance R$^'$ = I$_{sample}$ / I$_{(reference\ sample)}$.

A similar study was performed on a HPW12 sample which was beforehand saturated with NO/NO$_2$ at RT to provide a P-HPW12 sample, and then heated from RT to 380 °C at 3 °C/min under Ar(40%)/He (50 mL$_{NTP}$/min). At 380 °C, the P-HPW12 sample was exposed to an O$_2$-free feed of NO (~ 2000 ppm) in Ar(40%)/He (50 mL$_{NTP}$/min) (*in situ* DRIFT difference spectra shown in Figure S9, panel 1). The P-HPW12 sample was then purged under Ar(40%)/He (50 mL$_{NTP}$/min) before exposure to a feed of NO (~ 2000 ppm) in O$_2$(5%)-Ar(40%)/He (50 mL$_{NTP}$/min). Figure 7 shows the *in situ* DRIFT difference spectra of P-HPW12 at 380 °C as a function of time of exposure to the O$_2$-containing NO feed, in the spectral region of N=O stretches within NOH$^+$ and HNO$_2$$^+$ species. During the exposures to the two NO feeds at 380 °C, the difference spectra were obtained by subtraction of the last spectrum recorded at 380 °C under Ar(40%)/He before the respective NO feed was contacted with the P-HPW12 sample.

The difference spectra (d-spectra hereafter) recorded within the first 10 min under the O$_2$-free NO feed (Figure S9, panel 1) do not show the appearance of any IR absorption contribution. The d-spectrum recorded after 30 min on stream shows the appearance of a slight negative band at 2261 cm^{-1}, which was found to remain essentially unchanged at longer exposures to the O$_2$-free NO feed (d-spectra at 60 and 80 min in Figure S9, panel 1). In contrast, on the d-spectra recorded under the O$_2$-containing NO feed (Figure 7), a sharp negative band was quickly observed at 2261 cm^{-1} (d-spectrum at 2 min). The area of

this band then continuously decreased until the end of the experiment (d-spectra from 4 to 900 min, Figure 7). From 2 to 34 min on stream, it remained higher than that on the last d-spectrum recorded under the O_2-free NO feed (Figure S9, panel 2 *vs*. panel 1). At longer exposures to the O_2-containing NO feed (d-spectra from 60 min in Figure 7), the area of the band at 2261 cm^{-1} became lower than that on the last d-spectrum recorded under the O_2-free NO feed (Figure S9, panel 1), without however reaching zero on the final spectrum at 900 min on stream.

The negative band at 2261 cm^{-1} indicates the disappearance of NOH^+ and/or HNO_2^+ species which had been stored in the bulk of the sample during its pre-exposure to NO_x at RT, due to their desorption and/or reaction under the $NO-O_2$ containing feed. The limited disappearance of pre-absorbed NOH^+ and/or HNO_2^+ species under the O_2-free NO feed (Figure S9, panel 1) can be attributed to the slight desorption of such species in agreement with the release of NO_x species recorded in Figure 4a and the absence of N_2 formation (Figure 4b). In contrast, the sharp disappearance of pre-absorbed NOH^+ and/or HNO_2^+ species under the O_2-containing feed (Figure 7) is rather attributed to their reaction as supported by the presence of N_2 in the effluent of the corresponding NO decomposition experiment described in section 3.2 (Figure 5c). The latter experiment showed that the presence of O_2 in the reaction feed allowed NO_x from the latter feed to enter into the bulk of the sample, which led to NO_x decomposition into N_2. The present DRIFT results show that this decomposition process relied on both the NO_x from the feed and the NO_x species pre-absorbed in the bulk. The NO_x from the feed reacted over the HPW12 units with the involvement of pre-absorbed NOH^+ species ($NO_{gas} + NOH^+ = N_2 + O_2 + H^+$, or $NO_{gas} + H^+ = NOH^+$ followed by $NOH^+ + NOH^+ = N_2 + O_2 + 2 H^+$). The involvement of pre-absorbed HNO_2^+ species seems unlikely in view of the deactivating impact of NO_2 demonstrated in section 3.3.2. Hence, the present data suggest that NOH^+ species are important intermediates in the direct decomposition of NO_x over HPW12 at 380 °C, which thus relies on the protons of HPW12.

The fact that the band at 2261 cm^{-1} became less and less negative with increasing time on stream under the O_2-containing NO feed (Figure 7) indicates that unreactive NOH^+ and/or HNO_2^+ species were formed/adsorbed on the HPW12 units along with the reaction of pre-absorbed NOH^+ species with NO_x from the feed. This accumulation of unreactive NOH^+ and/or HNO_2^+ species may have occurred according to two non-exclusive mechanisms. Firstly, along with the consumption of NOH^+ species through their reaction with NO_x from the feed, the regenerated protons might have been poisoned with NO_2 by forming unreactive HNO_2^+ species. Secondly, considering that the lacunary heteropolyanions might act as reductants in the direct decomposition of NO_x over HPW12, as proposed earlier in section 3.1.2, NO_2 and/or O_2 might have oxidized the heteropolyanions, thereby making them non-reductive and thus inactive in the direct decomposition of NO_x from the feed, and leading to the accumulation of NOH^+ species which were no longer able to react. Through the first and/or the second mechanism, this accumulation of unreactive species finally contributed to the deactivation of P-HPW12 observed in section 3.3.2 (Figures 5a-b and S8).
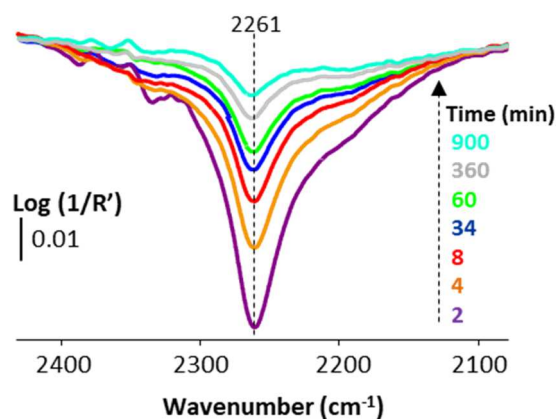
Figure 7. *In situ* DRIFT difference spectra of P-HPW12 (P standing for NO_x-pre-saturated) at 380 °C *vs.* time of exposure to a feed of NO (~ 2000 ppm) in O_2(5%)-Ar(40%)/He (50 mL_{NTP}/min), in the spectral region of N=O stretches within NOH^+ and HNO_2^+ species. P-HPW12 was heated from RT to 380 °C at 3 °C/min under Ar(40%)/He (50 mL_{NTP}/min). All difference spectra were obtained by subtraction of the last spectrum at 380 °C under Ar(40%)/He measured before NO and O_2 were added into the feed. Log (1/R') is expressed in arbitrary units, with the relative reflectance $R' = I_{sample} / I_{(reference\ sample)}$.

4. Conclusions

For the first time, the activity of $H_3PW_{12}O_{40}$ (HPW12) in the direct decomposition of NO_x was investigated under continuous NO_x feeding, at 380 °C. From the recorded NO decomposition and *in situ* DRIFT data, the observed NO_x decomposition activity of HPW12 was deduced to occur either through the reaction of two neighbouring NOH^+ adspecies, or through the reaction of one NOH^+ adspecies with gas phase NO. The presence of NO_2 – either in the reaction feed due to the presence of O_2 or in the bulk of the sample – was found to deactivate HPW12, likely because NO_2 poisoned the protons by forming unreactive HNO_2^+ species. Nevertheless, the presence of O_2 – in the feed and/or generated by the decomposition process – was also found to have a positive impact, namely to initiate the diffusion of NO_x into the bulk of the HPW12 crystals. However, this diffusion process effectively took place only when the bulk of HPW12 already contained NO_x beforehand pre-absorbed at RT, i.e. when the HPW12 crystals were still hydrated. Indeed, at 380 °C, the pre-absorbed NO_x species preserved the diffusion pathway in-between the bulk HPW12 units and therefore allowed the diffusion of the NO_x from the feed and their reaction with NOH^+ species. In the presence of O_2 in the feed, the bulk-type reaction allowed the otherwise inactive HPW12 material to remain active for 8 hours. By providing the key parameters involved in the NO_x decomposition process over HPW12 at 380 °C, the present work paves the way for future investigations in order to further improve the lifetime and activity of HPW12. Future investigations may focus, for instance, on tuning the chemical composition of the surface and/or bulk heteropolyanions in order to make the HPA more resistant to poisoning by O_2 and/or NO_2.

Supporting information

Structural water desorption profiles upon heating the two HPW12 samples from RT to the reaction temperature 380 °C under inert atmosphere; Full *in situ* DRIFT absorbance spectra of the two HPW12

22

samples under various conditions; NO and NO_2 concentrations and N_2/Ar trace recorded *vs.* time on stream in the blank NO decomposition experiments with only quartz wool in the reactor; H_2O concentration recorded *vs.* time on stream during the pre-saturation of P-HPW12 with NO_x at RT; NO and NO_2 concentrations and N_2/Ar trace recorded *vs.* time on stream upon heating P-HPW12 from RT to the reaction temperature 380 °C under inert atmosphere; Comparison of the NO and NO_2 concentrations recorded *vs.* time on stream in the two successive NO decomposition experiments over P-HPW12 at 380 °C in the absence of O_2 in the feed; N_2/Ar trace recorded *vs.* time on stream in the NO decomposition experiment over P-HPW12 at 380 °C in the presence of O_2 in the feed, over a longer time scale (600 min) than shown in the manuscript (30 min); Detailed comparison of the *in situ* DRIFT difference spectra in the region of N=O stretches within NOH^+ and HNO_2^+ species measured in the experiments over P-HPW12 at 380 °C in the absence *vs.* presence of O_2 in the feed.

Acknowledgements

Author information

Corresponding authors
*E-mails: josefine.schnee@upmc.fr, josischnee@hotmail.com, cyril.thomas@upmc.fr.

ORCID numbers
Josefine Schnee: 0000-0001-8521-9922

Laurent Delannoy: 0000-0002-3263-5065

Guylène Costentin: 0000-0003-1559-6890

Cyril Thomas: 0000-0003-4224-6095

Competing interests

The authors declare no competing interests.

References

1.   Kozhevnikov, I. V. Sustainable heterogeneous acid catalysis by heteropoly acids. *J. Mol. Catal. A: Chem.* **2007,** *262*, 86-92.

2.   Kozhevnikov, I. V. Catalysis by heteropoly acids and multicomponent polyoxometalates in liquid-phase reactions. *Chem. Rev.* **1998,** *98*, 171-198.

3.   Ganapathy, S.; Fournier, M.; Paul, J. F.; Delevoye, L.; Guelton, M.; Amoureux, J. P. Location of protons in anhydrous Keggin heteropolyacids $H_3PMo_{12}O_{40}$ and $H_3PW_{12}O_{40}$ by 1H{31P}/31P{1H} REDOR NMR and DFT quantum chemical calculations. *J. Amer. Chem. Soc.* **2002,** *124*, 7821-7828.

4.   Li, G.; Ding, Y.; Wang, J.; Wang, X.; Suo, J. New progress of Keggin and Wells–Dawson type polyoxometalates catalyze acid and oxidative reactions. *J. Mol. Catal. A: Chem.* **2007,** *262*, 67-76.

5.   Bielański, A.; Lubańska, A.; Micek-Ilnicka, A.; Poźniczek, J. Polyoxometalates as the catalysts for tertiary ethers MTBE and ETBE synthesis. *Coord. Chem. Rev.* **2005,** *249*, 2222-2231.

6.   Janik, M. J.; Campbell, K. A.; Bardin, B. B.; Davis, R. J.; Neurock, M. A computational and experimental study of anhydrous phosphotungstic acid and its interaction with water molecules. *Appl. Catal., A* **2003,** *256*, 51-68.

7.   Zhang, H.; Zheng, A.; Yu, H.; Li, S.; Lu, X.; Deng, F. Formation, location, and photocatalytic reactivity of methoxy species on Keggin 12-$H_3PW_{12}O_{40}$: A joint solid-state NMR spectroscopy and DFT calculation study. *J. Phys. Chem. C* **2008,** *112*, 15765-15770.

8.   Sugii, T.; Ohnishi, R.; Zhang, J.; Miyaji, A.; Kamiya, Y.; Okuhara, T. Acidity-attenuated heteropolyacid catalysts: Acidity measurement using benzonitrile-TPD and catalytic performance in the skeletal isomerization of n-heptane. *Catal. Today* **2006,** *116*, 179-183.

9.   Chen, N.; Yang, R. T. Activation of nitric oxide by heteropoly compounds: Structure of nitric-oxide linkages in tungstophosphoric acid with Keggin units. *J. Catal.* **1995,** *157*, 76-86.

10.   Reddy, G. K.; Ling, C.; Peck, T. C.; Jia, H. Understanding the chemical state of palladium during the direct NO decomposition – influence of pretreatment environment and reaction temperature. *RSC Adv.* **2017,** *7*, 19645-19655.

11.   Haneda, M.; Hamada, H. Recent progress in catalytic NO decomposition. *C. R. Chim.* **2016,** *19*, 1254-1265.

12.   Reddy, G. K.; Peck, T. C.; Roberts, C. A. CeO_2–M_xO_y (M = Fe, Co, Ni, and Cu)-based oxides for direct NO decomposition. *J. Phys. Chem. C* **2019,** *123*, 28695-28706.

13.   Imanaka, N.; Masui, T. Advances in direct NO_x decomposition catalysts. *Appl. Catal., A* **2012,** *431-432*, 1-8.

14.   Song, Y.-J.; Jesús, Y. M. L.-D.; Fanson, P. T.; Williams, C. T. Kinetic evaluation of direct NO decomposition and NO–CO reaction over dendrimer-derived bimetallic Ir–Au/Al_2O_3 catalysts. *Appl. Catal., B* **2014,** *154-155*, 62-72.

15.   Modén, B.; Da Costa, P.; Fonfé, B.; Lee, D. K.; Iglesia, E. Kinetics and mechanism of steady-state catalytic NO decomposition reactions on Cu–ZSM5. *J. Catal.* **2002,** *209*, 75-86.

16.   Wang, X.; Sigmon, S. M.; Spivey, J. J.; Lamb, H. H. Support and particle size effects on direct NO decomposition over platinum. *Catal. Today* **2004,** *96*, 11-20.

17.   Peck, T. C.; Reddy, G. K.; Roberts, C. A. Monolayer supported CuO_x/Co_3O_4 as an active and selective low temperature NO_x decomposition catalyst. *Catal. Sci. Technol.* **2019,** *9*, 1132-1140.

18. Kozhevnikov, I. V. Sustainable heterogeneous acid catalysis by heteropoly acids. *J. Mol. Catal. A: Chem.* **2007,** *262*, 86-92.

19. Herring, A. M.; McCormick, R. L. *In Situ* infrared study of the absorption of nitric oxide by 12-tungstophosphoric acid. *J. Phys. Chem. B* **1998,** *102*, 3175-3184.

20. Weng, X.; Dai, X.; Zeng, Q.; Liu, Y.; Wu, Z. DRIFT studies on promotion mechanism of $H_3PW_{12}O_{40}$ in selective catalytic reduction of NO with NH_3. *J. Colloid Interface Sci.* **2016,** *461*, 9-14.

21. Schnee, J.; Gaigneaux, E. M. Elucidating and exploiting the chemistry of Keggin heteropolyacids in the methanol-to-DME conversion: enabling the bulk reaction thanks to *operando* Raman. *Catal. Sci. Technol.* **2017,** *7*, 817-830.

22. Schnee, J.; Gaigneaux, E. M. Lifetime of the $H_3PW_{12}O_{40}$ heteropolyacid in the methanol-to-DME process: A question of pre-treatment. *Appl. Catal., A* **2017,** *538*, 174-180.

23. Yang, R. T.; Chen, N. A new approach to decomposition of nitric oxide using sorbent/catalyst without reducing gas: Use of heteropoly compounds. *Ind. Eng. Chem. Res.* **1994,** *33*, 825-831.

24. Sirita, J.; Phanichphant, S.; Meunier, F. C. Quantitative analysis of adsorbate concentrations by diffuse reflectance FT-IR. *Anal. Chem.* **2007,** *79*, 3912-3918.

25. Belanger, R.; Moffat, J. B. A comparative study of the adsorption and reaction of nitrogen oxides on 12-tungstophosphoric, 12-tungstosilicic, and 12-molybdophosphoric acids. *J. Catal.* **1995,** *152*, 179-188.

TOC image
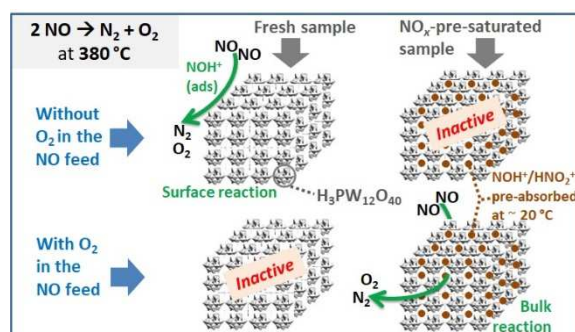
Unravelling the Direct Decomposition of NO$_x$ over Keggin Heteropolyacids and their Deactivation Using a Combination of Gas-IR/MS and *in Situ* DRIFT

Josefine Schnee,* Laurent Delannoy, Guylène Costentin, and Cyril Thomas*

Sorbonne Université, CNRS, Laboratoire de Réactivité de Surface (LRS), F-75005 Paris, France.

*Corresponding authors: josefine.schnee@upmc.fr, josischnee@hotmail.com, cyril.thomas@upmc.fr.
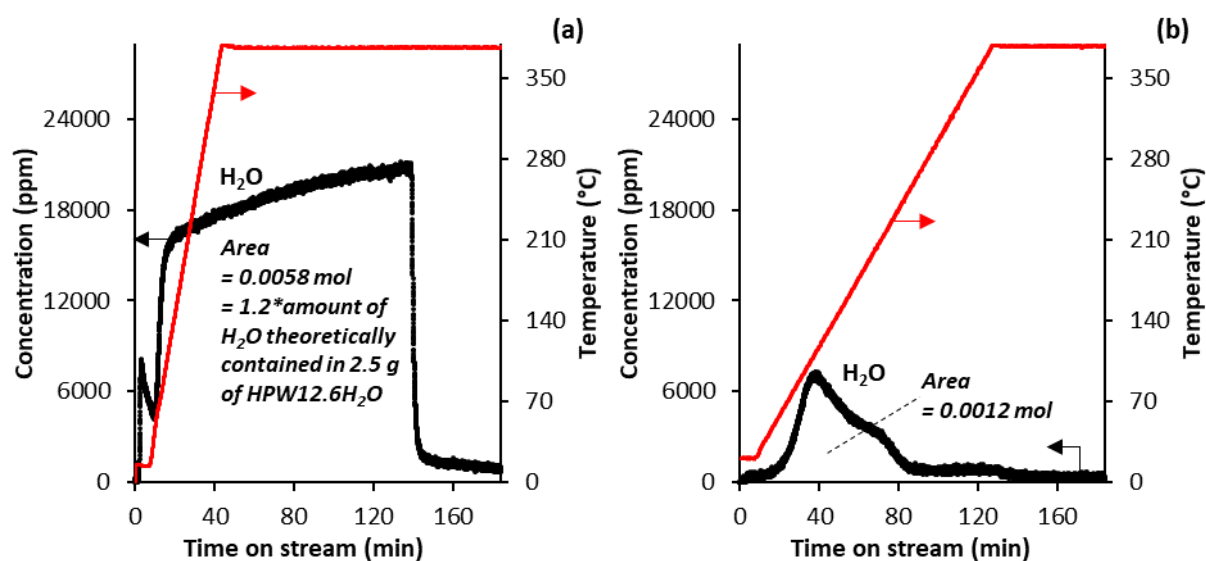
Supplementary information

Figure S1. H$_2$O concentration and temperature trace recorded by the MKS MultiGas 2030 IR analyzer as a function of time on stream upon heating (a) the N-HPW12 sample from RT to 380 °C at 10 °C/min under He (50 mL$_{NTP}$/min), and (b) the P-HPW12 sample from RT to 380 °C at 3 °C/min under Ar(8%)/He (50 mL$_{NTP}$/min).
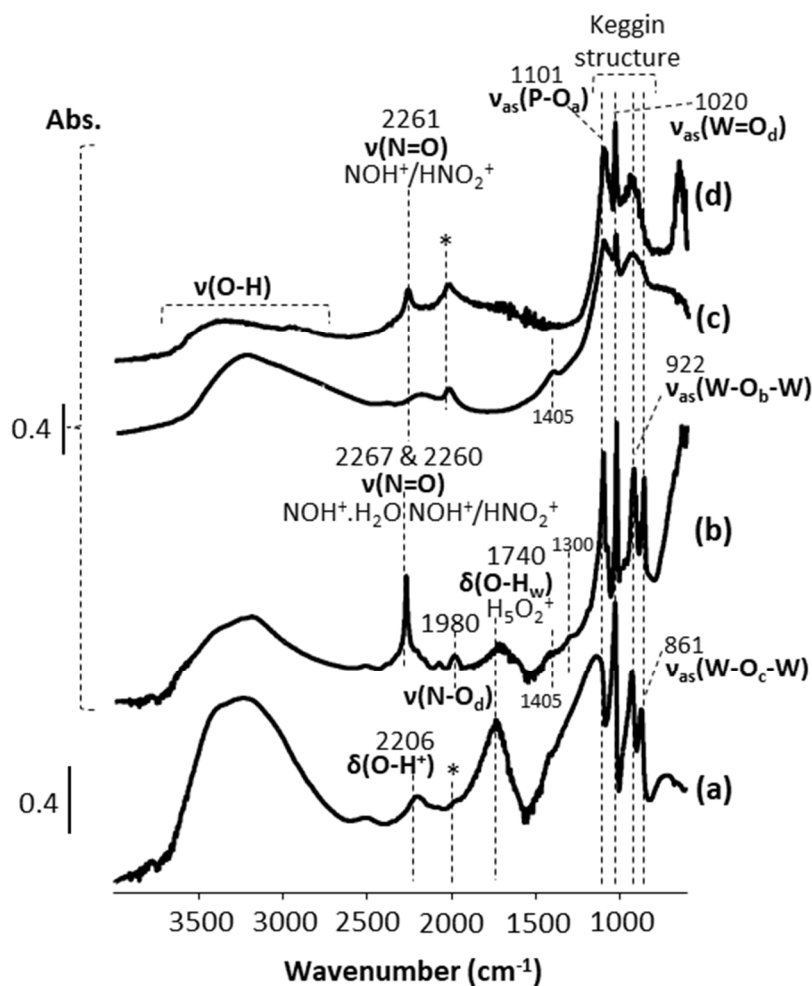
Figure S2. *In situ* DRIFT spectra of (a,c) N-HPW12 and (b,d) P-HPW12, at (a-b) RT and (c-d) 380 °C, under 50 mL$_{NTP}$/min of (a,c-d) Ar(40%)/He and (b) NO (~ 2000 ppm) in O$_2$(5%)-Ar(40%)/He (since 48 h, i.e. at the end of the pre-treatment yielding the P-HPW12 sample). Spectra (c) and (d) were measured after heating the samples from RT to 380 °C at 3 °C/min under Ar(40%)/He. "Abs." means absorbance, and it is expressed in arbitrary units. "O-H$_w$" means O-H within water. The band marked with a star (∗) on spectra (a), (c) and (d) is not attributed in the literature, to our knowledge. Within the fingerprint of the Keggin structure, due to a saturation effect, the bands are shifted to higher wavenumbers as compared to their equivalents on the spectra of HPW12 diluted (20 wt.%) in diamond powder measured in the same conditions (not shown). In agreement with the literature (Janik, M. J.; Campbell, K. A.; Bardin, B. B.; Davis, R. J.; Neurock, M., *Applied Catalysis A: General* **2003,** *256* (1-2), 51-68), the latter bands are positioned at 1080, 980, 885 and 790 cm^{-1}, respectively. Log (1/R) is expressed in arbitrary units, with the reflectance R = I$_{sample}$ / I$_{KBr}$. The weak bands at 1300 and 1405 cm^{-1} on spectra (b) and (c) are attributed to bidentate nitrate and nitrite species, respectively (Weng, X.; Dai, X.; Zeng, Q.; Liu, Y.; Wu, Z., *Journal of Colloid and Interface Science* **2016**, *461*, 9-14).
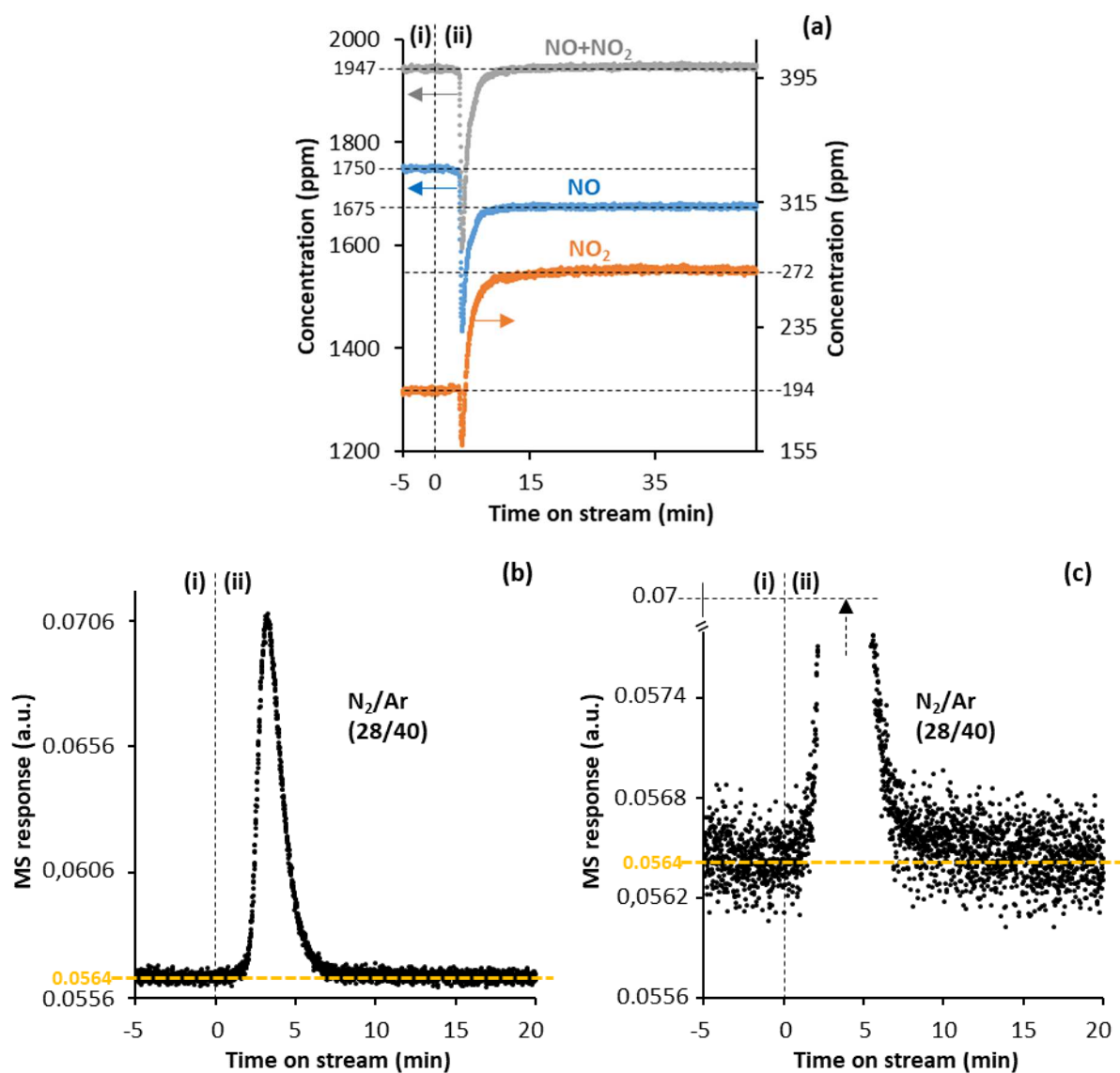
Figure S3. NO and NO$_2$ concentrations recorded by the MKS MultiGas 2030 IR analyzer (a) and mass to charge (m/z) ratio 28 associated with N$_2$ normalized by the m/z 40 one associated with Ar recorded by the MS (b-c) as a function of time on stream in the blank NO$_x$ decomposition experiment with only quartz wool in the reactor (no catalyst) at 380 °C and a reaction feed of NO (~ 2000 ppm) in O$_2$(5%)-Ar(13%)/He (50 mL$_{NTP}$/min). In (b) and (c), the same N$_2$/Ar trace is shown with two different y axis scales. In (i), the reaction feed was analyzed without flowing through the reactor (upon flowing exclusively through lines at RT). In (ii), the reaction feed was flowing through the reactor at 380 °C, and the outlet gas flow was analyzed over time-on-stream. In (a), the negative peaks centered at 10 min are attributed to the purge of the dead volume of the reactor upon introduction of the reaction feed. In (b) and (c), the N$_2$/Ar peak centered at 8 min is attributed to the release of air from the dead volume of the reactor, and/or to the introduction of air trapped in the valve that was turned for contacting the reaction feed with the sample. In (c), the upper intensity of this peak was cut from the graph, as indicated by the rising arrow.
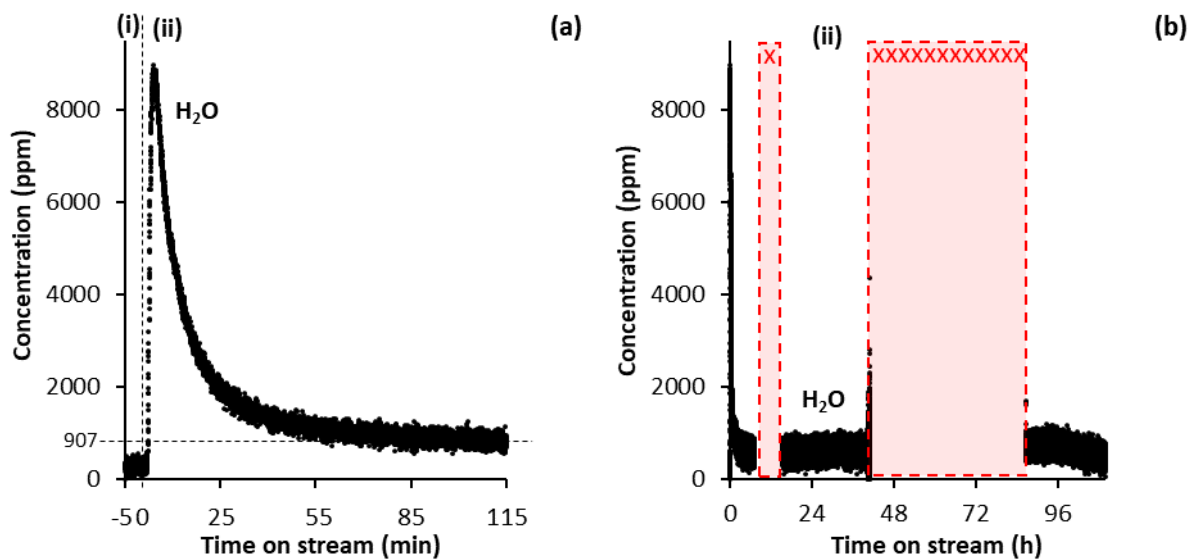
Figure S4. H_2O concentration recorded by the MKS MultiGas 2030 IR analyzer as a function of time on stream in the pre-exposure of HPW12 (2.5 g, < 125 µm) to a 50 mL$_{NTP}$/min feed of NO (~ 2000 ppm) in O_2(5%)-Ar(13%)/He at RT, to yield the P-HPW12 sample. In (i), the feed was analyzed without being contacted with the sample. In (ii), the feed was contacted with the sample, and the outlet gas flow was analyzed over time-on-stream. In (b), the same trace as in (a) is shown over a longer time scale. The periods marked with crosses (xxx) correspond to night and/or weekend periods in which the cryo-detector of the IR analyzer could not be filled with liquid N_2.
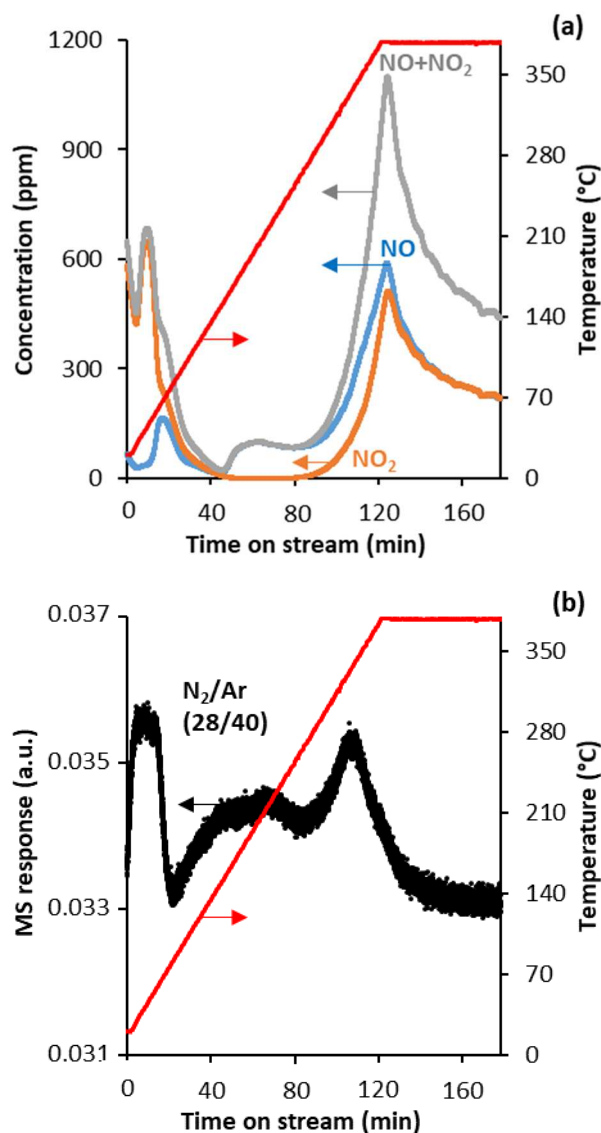
Figure S5. (a) NO and NO_2 concentrations and temperature trace recorded by the MKS MultiGas 2030 IR analyzer as a function of time on stream upon heating P-HPW12 (prepared by the treatment monitored in Figures 2 and S4) from RT to 380 °C at 3 °C/min under Ar(8%)/He (50 mL_{NTP}/min). The areas under the NO and NO_2 traces correspond to 7.42 x 10^{-5} mol of NO and 7.61 x 10^{-5} mol of NO_2, respectively. (b) In the same experiment, temperature trace recorded by the MKS MultiGas 2030 IR analyzer and mass to charge (m/z) ratio 28 associated with N_2 normalized by the m/z 40 one associated with Ar recorded by the MS.
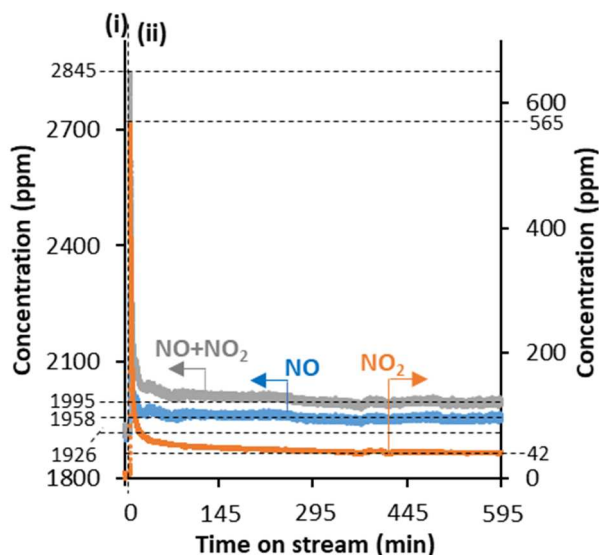
Figure S6. Same traces as those in Figure 4, but over a longer time scale – NO and NO_2 concentrations recorded by the MKS MultiGas 2030 IR analyzer *vs.* time on stream in the NO_x decomposition experiment with P-HPW12 (2.5 g, < 125 µm) at 380 °C and a reaction feed consisting of NO (~ 2000 ppm) in Ar(13%)/He (50 mL$_{NTP}$/min). In (i), the reaction feed was analyzed without being contacted with the sample (upon flowing exclusively through lines at RT). In (ii), the reaction feed was continuously contacted with the sample at 380 °C, and the outlet gas flow was analyzed over time on stream. P-HPW12 was heated from RT to 380 °C at 3 °C/min under Ar(8%)/He (50 mL$_{NTP}$/min).
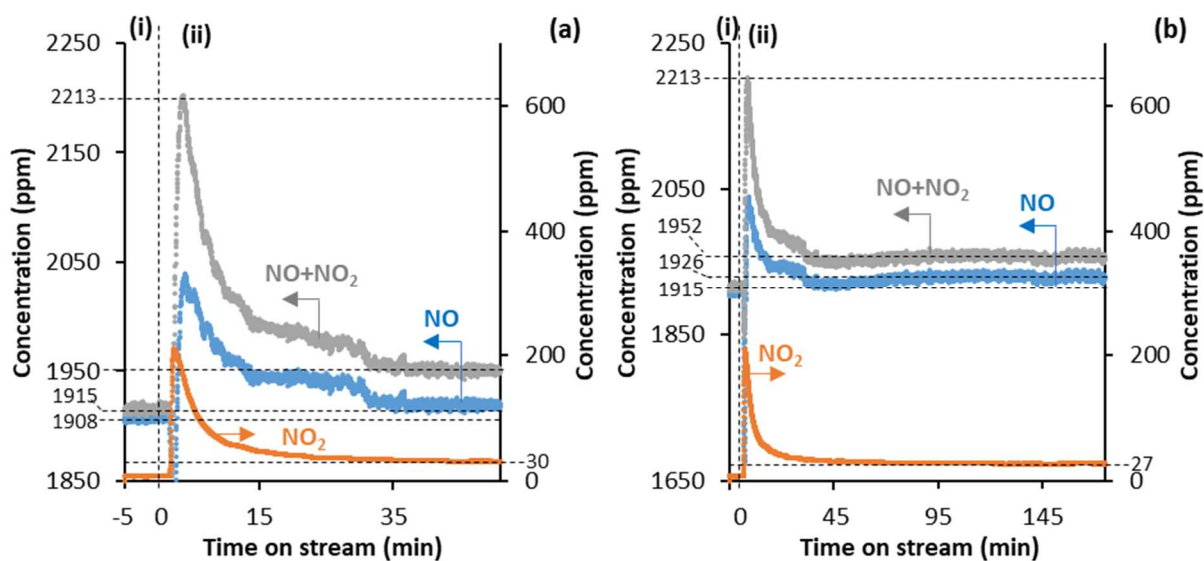

Figure S7. NO and NO_2 concentrations recorded by the MKS MultiGas 2030 IR analyzer *vs.* time on stream in the second NO_x decomposition experiment with P-HPW12 (2.5 g, < 125 µm) at 380 °C and a reaction feed consisting of NO (~ 2000 ppm) in Ar(13%)/He (50 mL$_{NTP}$/min). In (i), the reaction feed was analyzed without being contacted with the sample (upon flowing exclusively through lines at RT). In (ii), the reaction feed was continuously contacted with the sample at 380 °C, and the outlet gas flow was analyzed over time on stream. This experiment was launched after P-HPW12 had been purged for 10 h under He at 380 °C (50 mL$_{NTP}$/min) following the first NO_x decomposition experiment monitored in Figure S6.
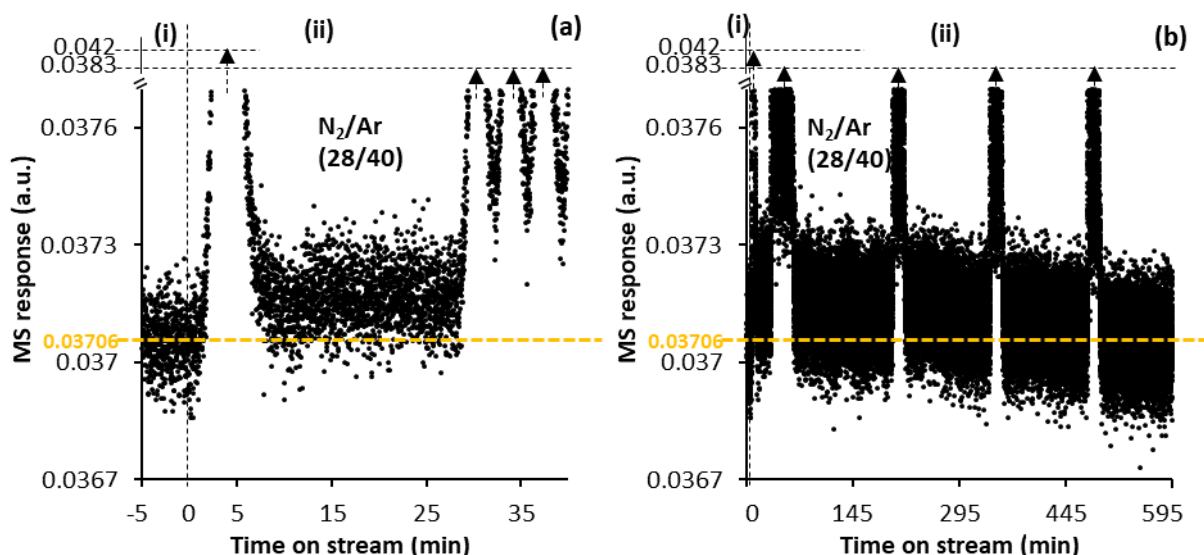
31

Figure S8. Same trace as that shown in Figure 5b, but over longer time scales, i.e. (a) 45 min and (b) 600 min. Mass to charge (m/z) ratio 28 associated with N_2 normalized by the m/z 40 one associated with Ar recorded by the MS as a function of time on stream in the NO_x decomposition experiment with P-HPW12 (2.5 g, < 125 µm) at 380 °C and a reaction feed of NO (~ 2000 ppm) in O_2(5%)-Ar(13%)/He (50 mL$_{NTP}$/min). In (i), the reaction feed was analyzed without being contacted with the sample (upon flowing exclusively through lines at RT). In (ii), the reaction feed was continuously contacted with the sample at 380 °C, and the outlet gas flow was analyzed over time-on-stream. P-HPW12 was heated from RT to 380 °C at 3 °C/min under Ar(8%)/He (50 mL$_{NTP}$/min). Except the first one attributed to the release of air trapped in the valve that served for contacting the reaction feed with the sample, the peaks marked with arrows are artifacts related to the simultaneously ongoing µ-GC analysis.
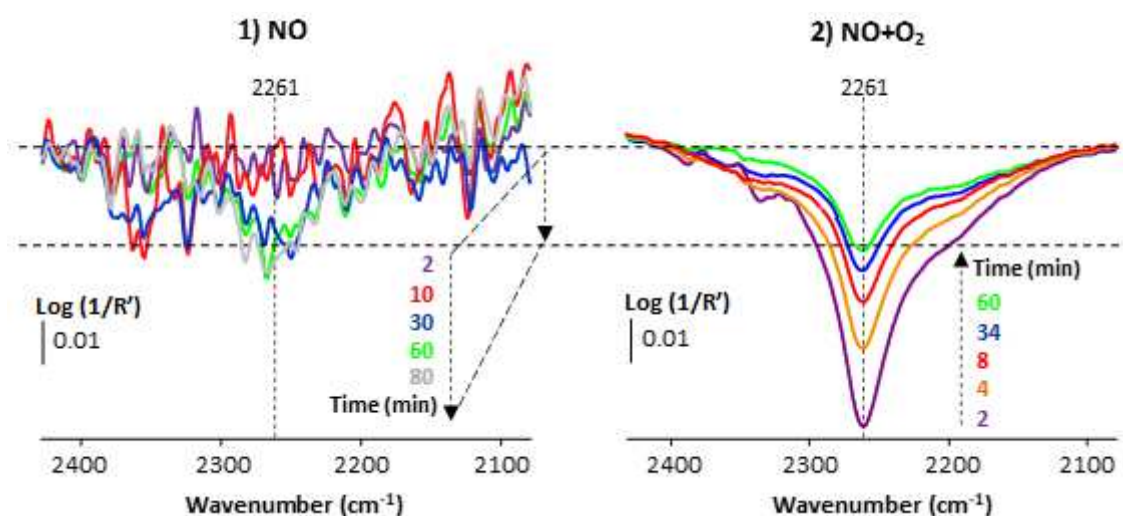

Figure S9. *In situ* DRIFT difference spectra of P-HPW12 at 380 °C *vs.* time of exposure to a feed of 1) NO (~ 2000 ppm) in Ar(40%)/He (50 mL$_{NTP}$/min) and subsequently 2) NO (~ 2000 ppm) in O_2(5%)-Ar(40%)/He (50 mL$_{NTP}$/min), in the spectral region of N=O stretches within NOH^+ and HNO_2^+ species. P-HPW12 was heated from RT to 380 °C at 3 °C/min under Ar(40%)/He (50 mL$_{NTP}$/min). The difference spectra were obtained by subtraction of the last spectrum at 380 °C under Ar(40%)/He measured before the reaction feed – NO without O_2 in step 1, *vs.* NO with O_2 in step 2 – was contacted with the P-HPW12 sample. The low signal to noise ratio of the spectra recorded in the absence of O_2 in the feed is attributed to the presence of water in the atmosphere of the spectrometer due to a reduced purge. Log (1/R') is expressed in arbitrary units, with the relative reflectance R' = I$_{sample}$ / I$_{(reference\ sample)}$.